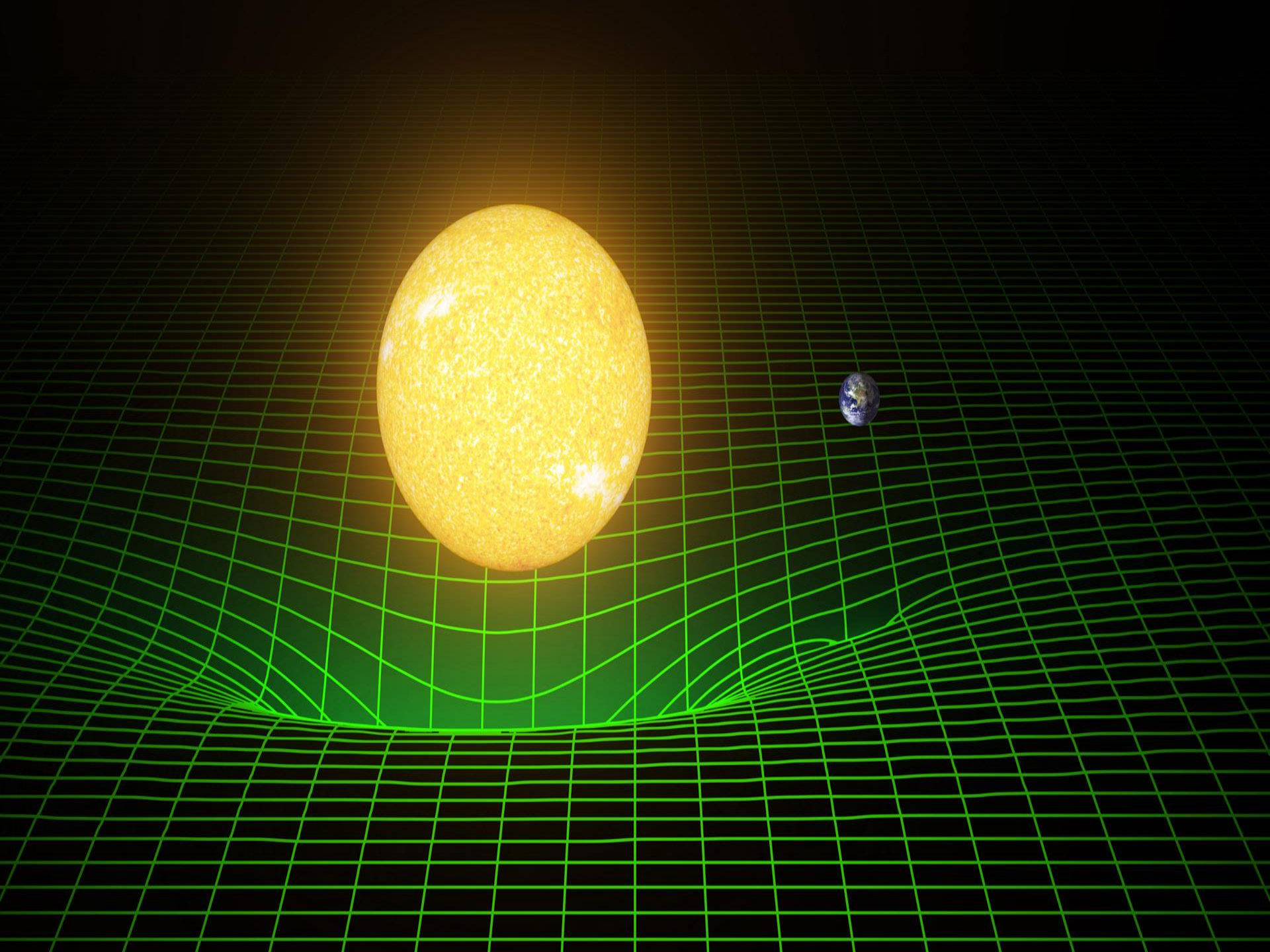


Observation of the merger of binary black holes: The opening of gravitational wave astronomy

R. Weiss, MIT, on behalf of the LIGO Scientific Collaboration

Fermi National Accelerator Laboratory

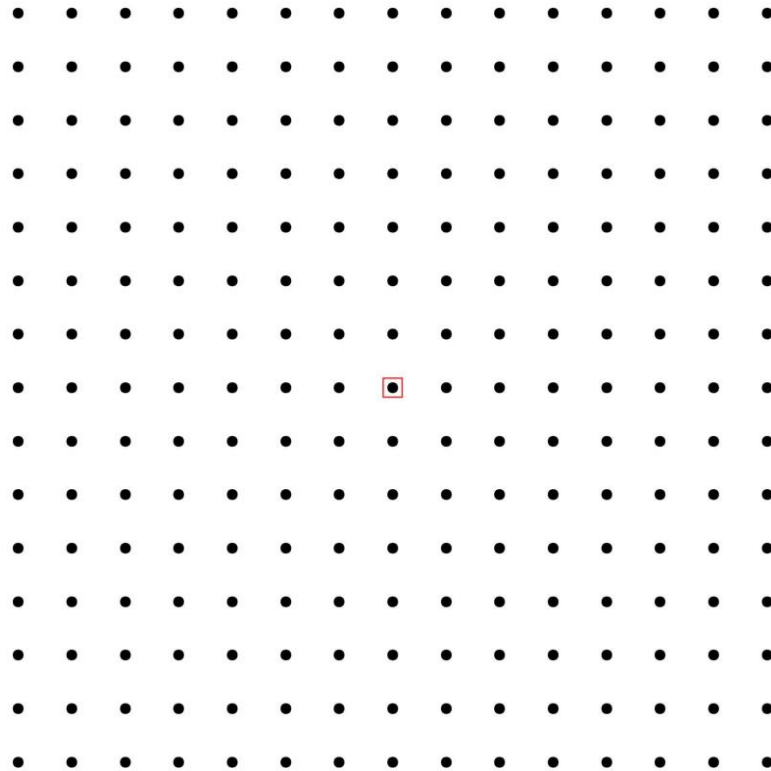
July 19, 2017



Gravitational waves

Einstein 1916 and 1918

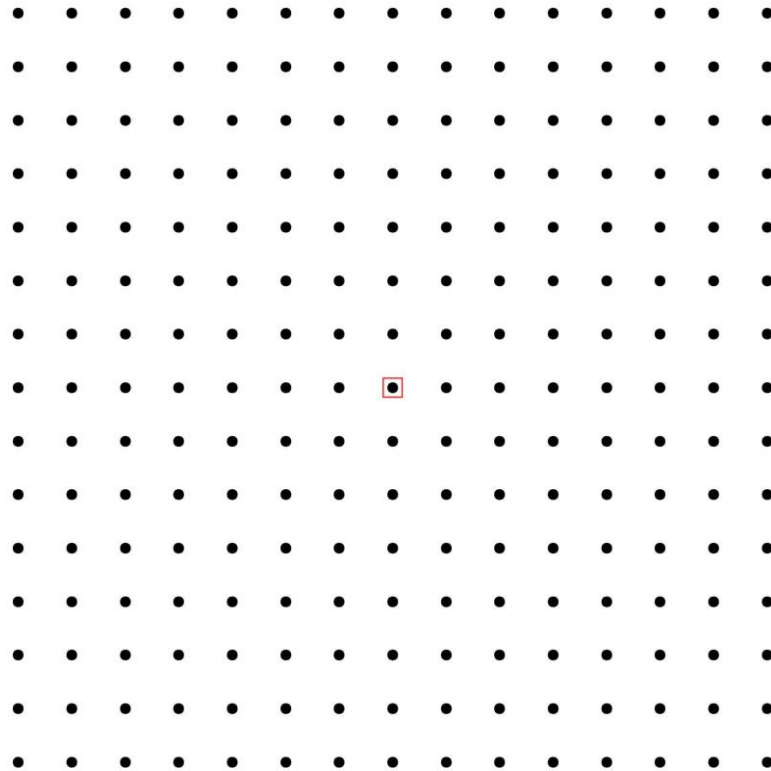
- Sources: non-spherically symmetric accelerated masses
- Kinematics:
 - propagate at speed of light
 - transverse waves, strains in space (tension and compression)



Gravitational waves

Einstein 1916 and 1918

- Sources: non-spherically symmetric accelerated masses
- Kinematics:
 - propagate at speed of light
 - transverse waves, strains in space (tension and compression)



Einstein 1916

$$A = \frac{\kappa}{24\pi} \sum_{\alpha\beta} \left(\frac{\partial^3 J_{\alpha\beta}}{\partial t^3} \right)^2. \quad (21)$$

Würde man die Zeit in Sekunden, die Energie in Erg messen, so würde zu diesem Ausdruck der Zahlenfaktor $\frac{1}{c^4}$ hinzutreten. Berücksichtigt man außerdem, daß $\kappa = 1.87 \cdot 10^{-27}$, so sieht man, daß A in allen nur denkbaren Fällen einen praktisch verschwindenden Wert haben muß. “....in any case one can think of A will have a practically vanishing value.”

$$h \gg \frac{j_{\text{Newton}}}{c^2} \frac{v^2}{c^2} = \frac{Gm}{Rc^2} \frac{v^2}{c^2} \quad S_g = \frac{c^3}{16\pi G} \langle \dot{h}_+^2 + \dot{h}_x^2 \rangle \quad \frac{c^3}{16\pi G} = 7.8 \times 10^{36} \text{ erg sec/cm}^2$$

1916 examples: **train collision**

binary star decay

$$\begin{aligned} m &= 10^5 \text{ kg} \\ v &= 100 \text{ km/hr} \\ T_{\text{collision}} &= 1/3 \text{ sec} \\ R_{\text{radiation}} &= 300 \text{ km} \\ h &\sim 10^{-42} \end{aligned}$$



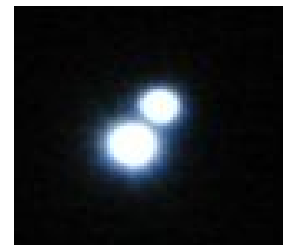
$$m_1 = m_2 = 1 \text{ solar mass}$$

$$T_{\text{orbit}} = 1 \text{ day}$$

$$R = 10 \text{ Kly}$$

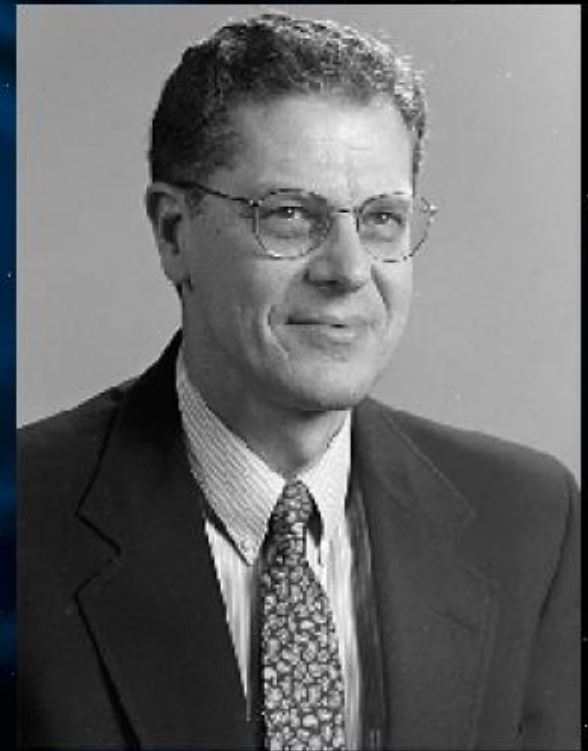
$$h \sim 10^{-23} \text{ @ } 1/2 \text{ day period}$$

$$Q = \frac{2\pi E_{\text{stored}}}{\Delta E_{1\text{period}}} \sim 10^{15} \quad \text{decaytime} \sim 10^{13} \text{ years}$$





Russel A. Hulse



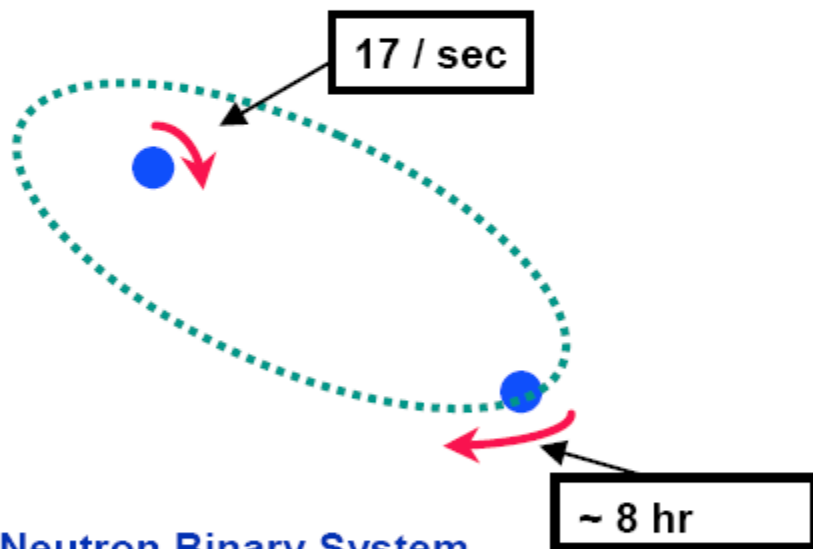
Joseph H. Taylor Jr

Gravitational Waves

the evidence

Neutron Binary System – Hulse & Taylor

PSR 1913 + 16 -- Timing of pulsars



Neutron Binary System

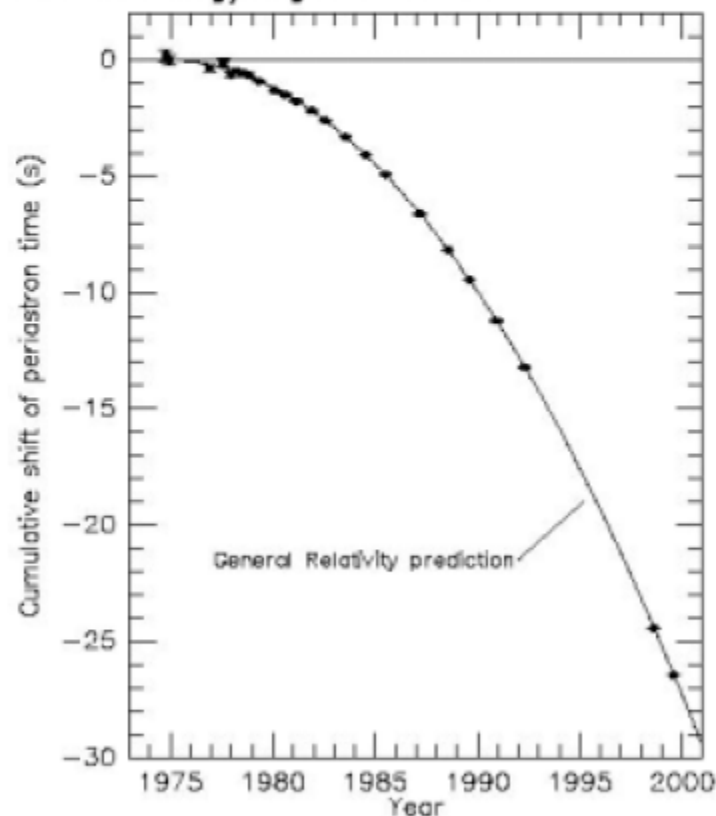
- separated by 10^6 miles
- $m_1 = 1.4m_{\odot}$; $m_2 = 1.36m_{\odot}$; $\epsilon = 0.617$

Prediction from general relativity

- spiral in by 3 mm/orbit
- rate of change orbital period

Emission of gravitational waves

Comparison between observations of the binary pulsar PSR1913+16, and the prediction of general relativity based on loss of orbital energy via gravitational waves



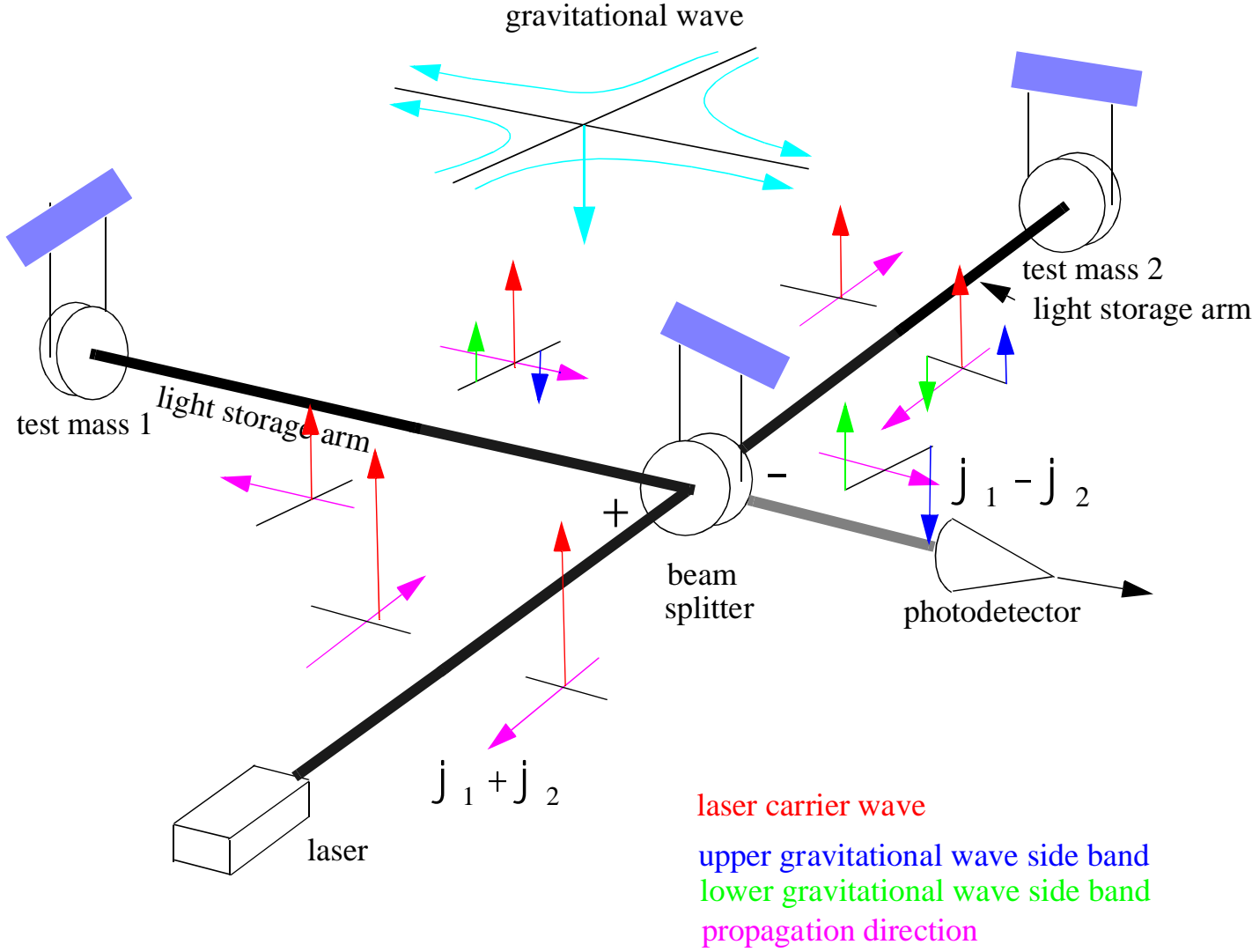
From J. H. Taylor and J. M. Weisberg, unpublished (2000)



Joseph Weber 1919-2000



Michelson Interferometer Schematic and GW sidebands



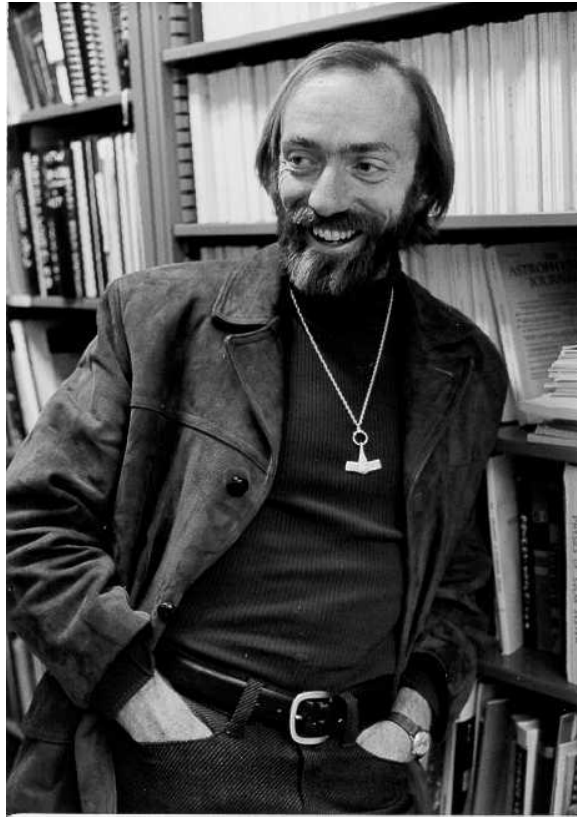
The measurement challenge

$$h = \frac{DL}{L} \leq 10^{-21}$$

$$L = 4\text{km} \quad DL \leq 4 \times 10^{-18} \text{ meters}$$

DL 10^{-12} wavelength of light

DL 10^{-12} vibrations at earth's surface



Kip Thorne

Initial interferometric GW detector groups late 1970's



H. Billing

Max Planck Garching



L. Schnupp



K. Maischberger



W. Winkler



R. Schilling



A. Rudiger



Glasgow

R. Drever



J. Hough



B. Meers

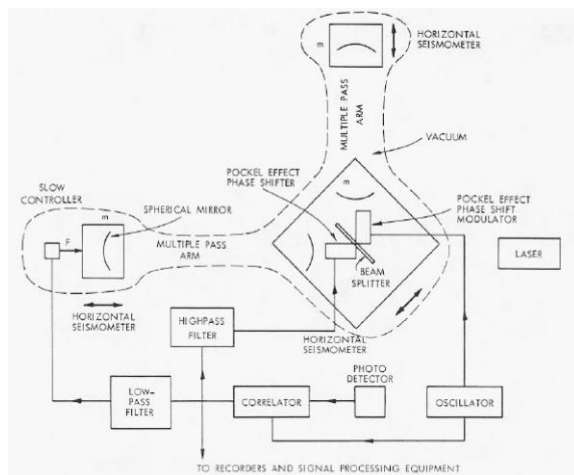


H. Ward



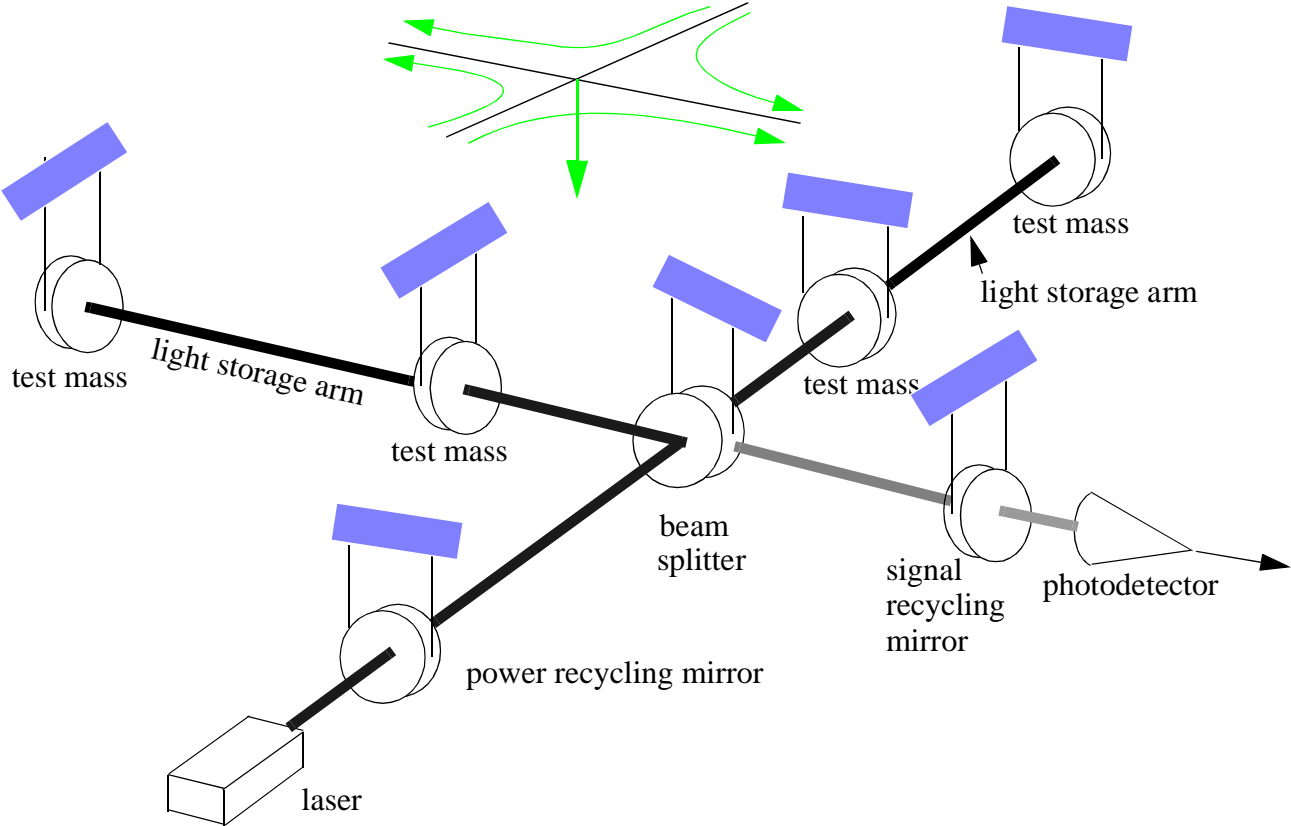
F.A.E. Pirani

MIT



J. Livas, D.H. Shoemaker, D. Dewey

Advanced LIGO Fabry-Perot Michelson Interferometer Schematic





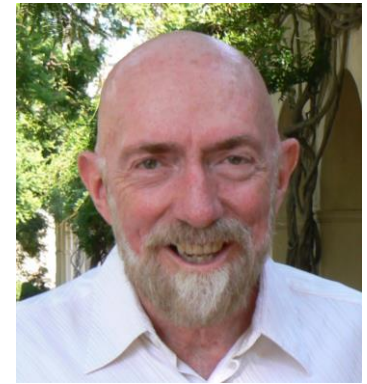
R. Drever



R. Vogt



W. Althouse



K. Thorne



F. Raab



F. Asiri



R. Savage



J. Worden



M. Zucker



L. Jones

Proposal to the National Science Foundation

**THE CONSTRUCTION, OPERATION, AND
SUPPORTING RESEARCH AND DEVELOPMENT
OF A**

**LASER INTERFEROMETER
GRAVITATIONAL-WAVE
OBSERVATORY**

*Submitted by the
CALIFORNIA INSTITUTE OF TECHNOLOGY
Copyright © 1989*

Rochus E. Vogt
Principal Investigator and Project Director
California Institute of Technology

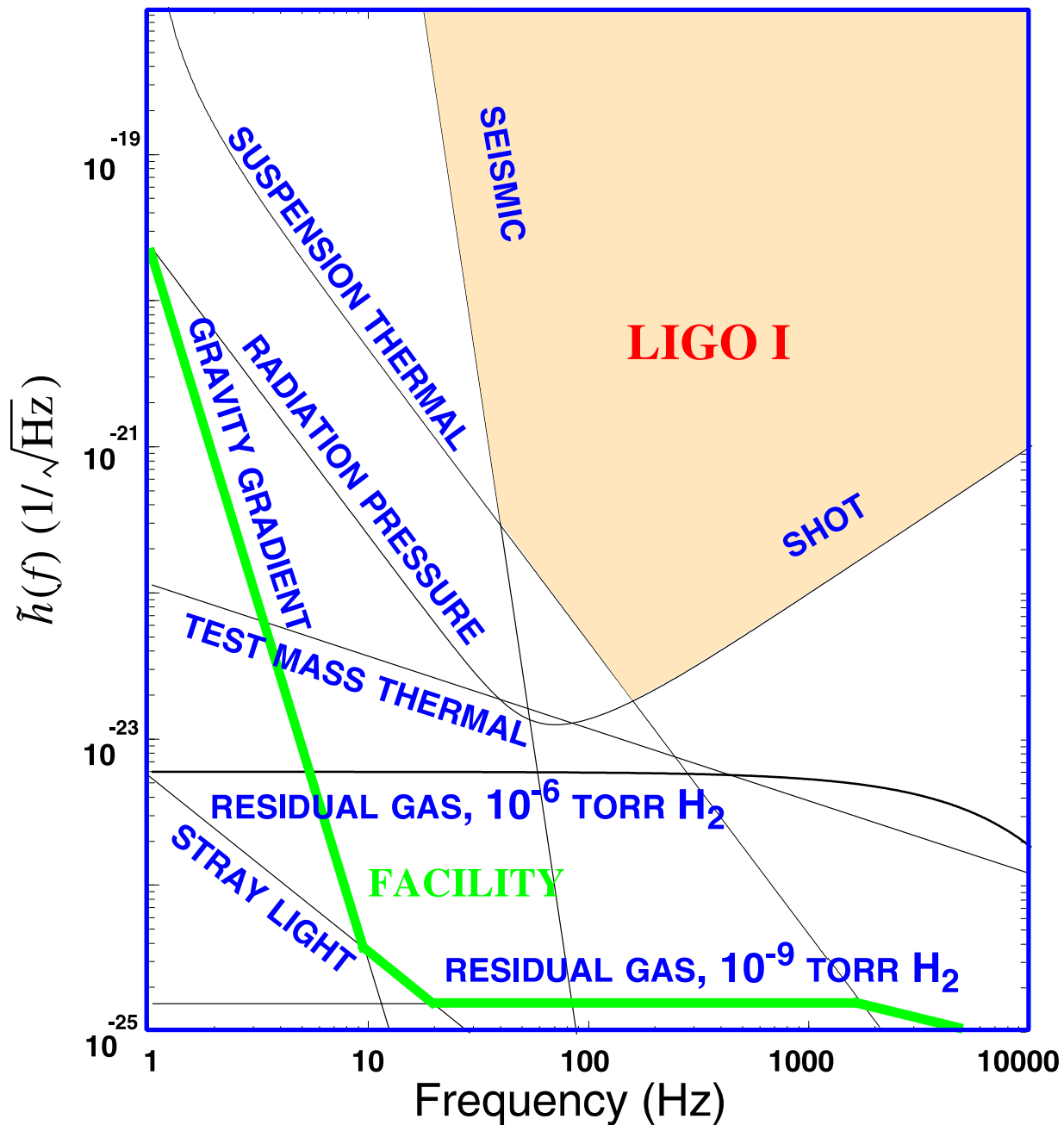
Ronald W. P. Drever
Co-Investigator
California Institute of Technology

Frederick J. Raab
Co-Investigator
California Institute of Technology

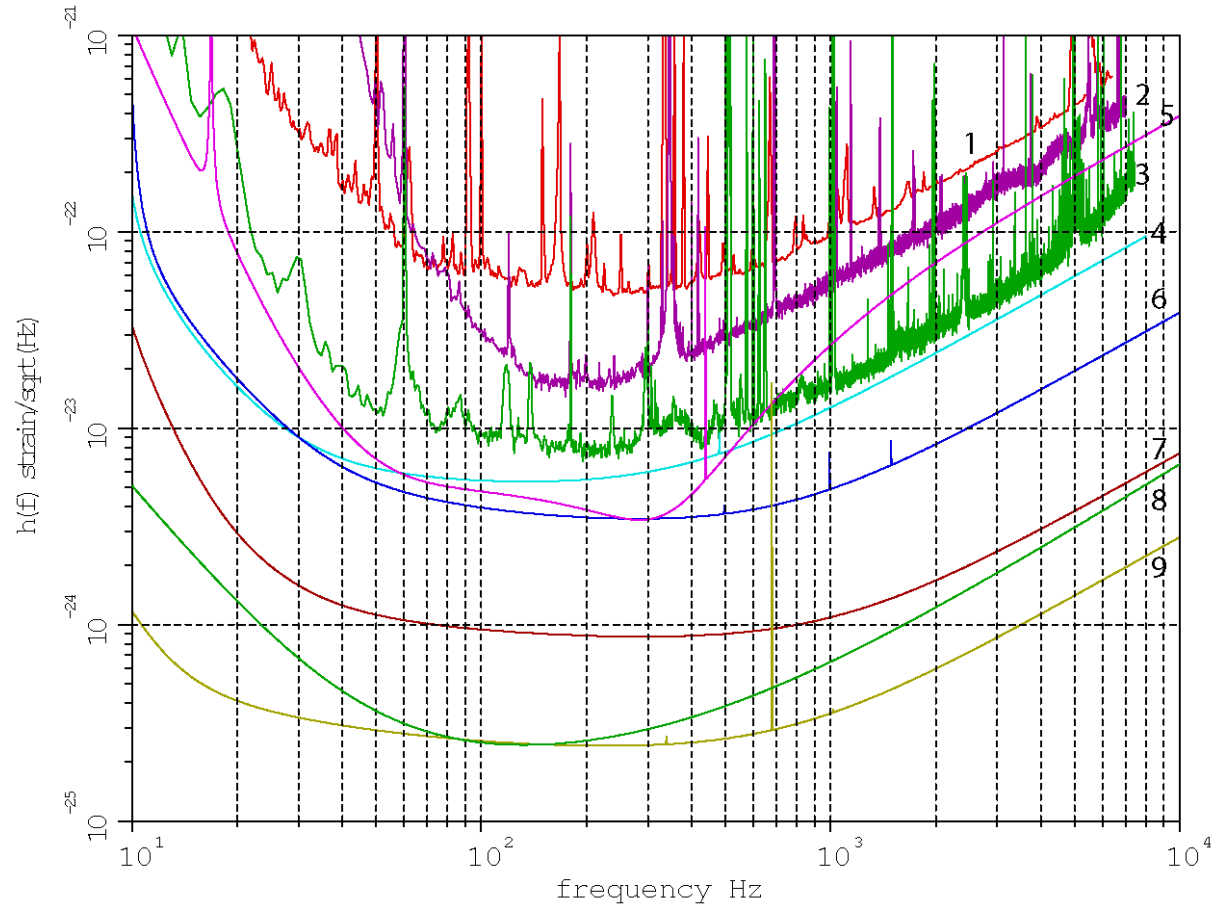
Kip S. Thorne
Co-Investigator
California Institute of Technology

Rainer Weiss
Co-Investigator
Massachusetts Institute of Technology

Initial LIGO Interferometer Noise Budget



Evolution of gravitational strain sensitivity



- 1 VIRGO 2009
- 2 Enhanced LIGO 2009
- 3 Advanced LIGO 65Mpc NS/NS 2015
- 4 Advanced LIGO 150Mpc NS/NS Low Power
- 5 Advanced VIRGO
- 6 Advanced LIGO 190Mpc NS/NS High Power
- 7 4km "Voyager" example 600Mpc NS/NS
- 8 Einstein telescope B
- 9 40km "Cosmic Explorer" example

Epoch	Estimated Run Duration	$E_{\text{GW}} = 10^{-2} M_{\odot} c^2$ Burst Range (Mpc)		BNS Range (Mpc)		Number of BNS Detections	% BNS Localized within	
		LIGO	Virgo	LIGO	Virgo		5 deg ²	20 deg ²
2015	3 months	40 – 60	–	40 – 80	–	0.0004 – 3	–	–
2016–17	6 months	60 – 75	20 – 40	80 – 120	20 – 60	0.006 – 20	2	5 – 12
2017–18	9 months	75 – 90	40 – 50	120 – 170	60 – 85	0.04 – 100	1 – 2	10 – 12
2019+	(per year)	105	40 – 80	200	65 – 130	0.2 – 200	3 – 8	8 – 28
2022+ (India)	(per year)	105	80	200	130	0.4 – 400	17	48

LHO



GEO



KAGRA

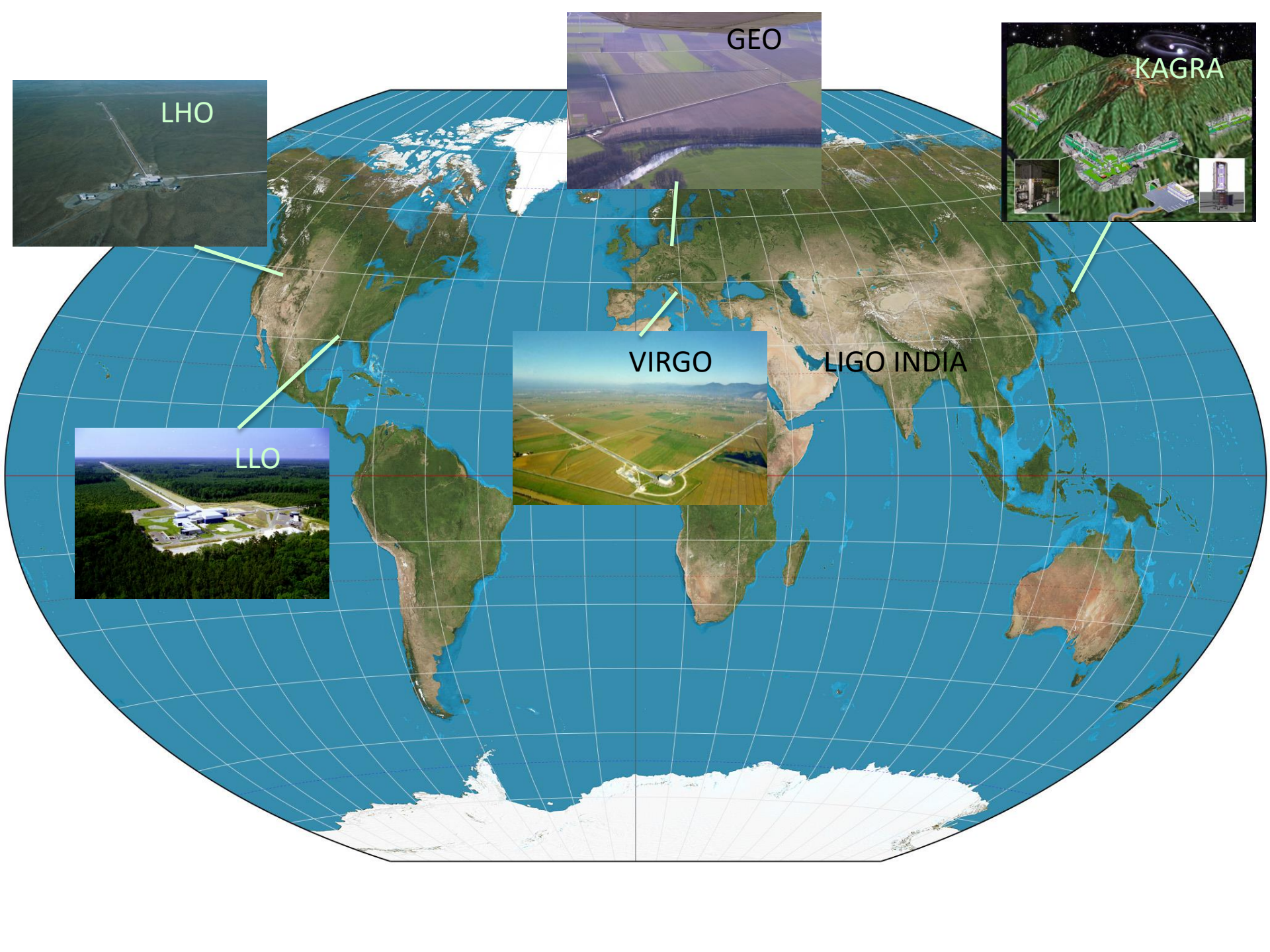


VIRGO



LIGO INDIA

LLO





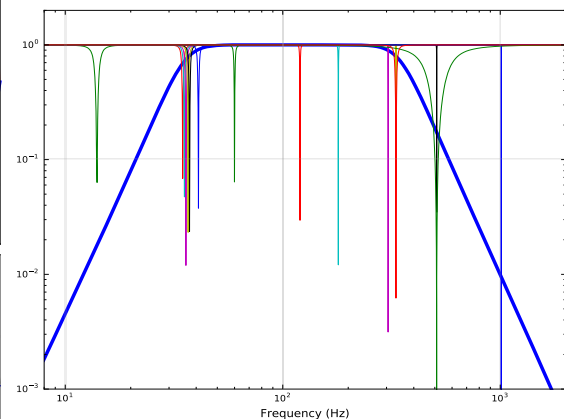
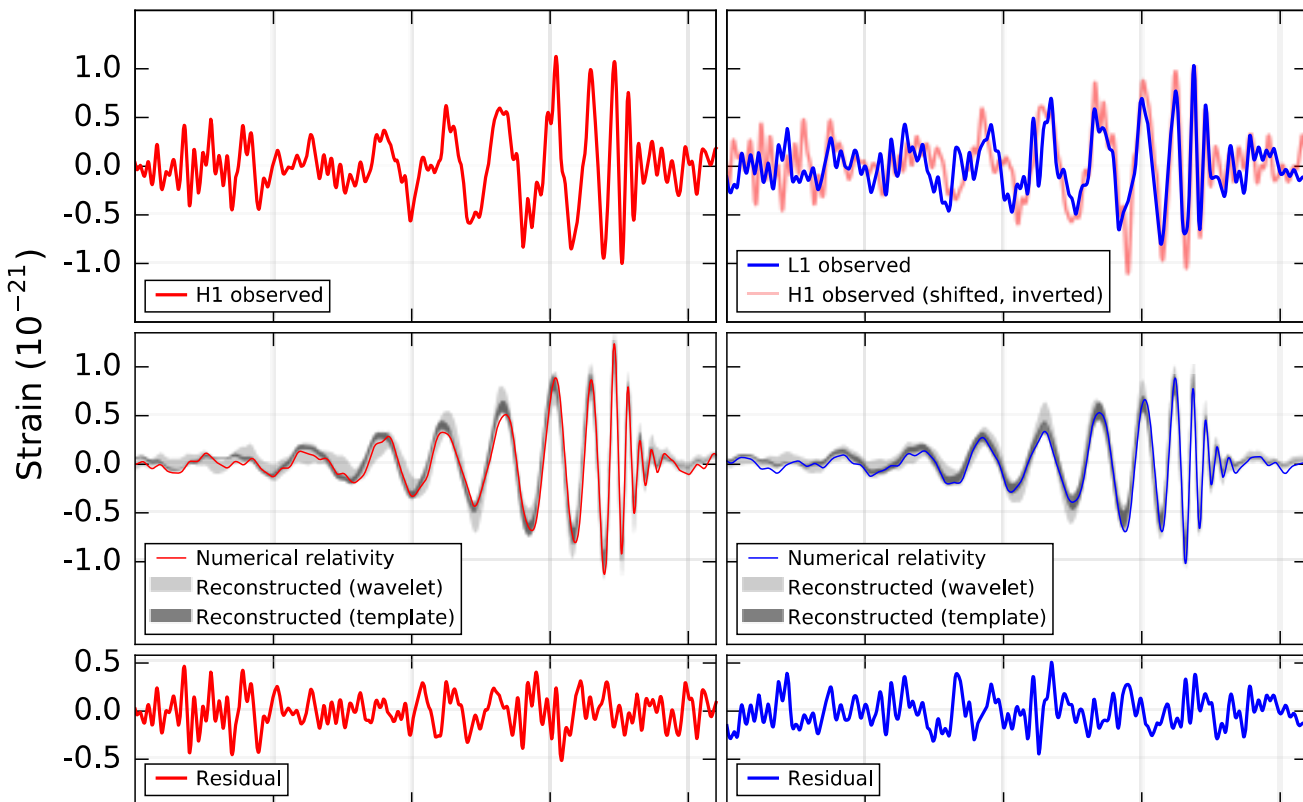


Criteria for transient detection

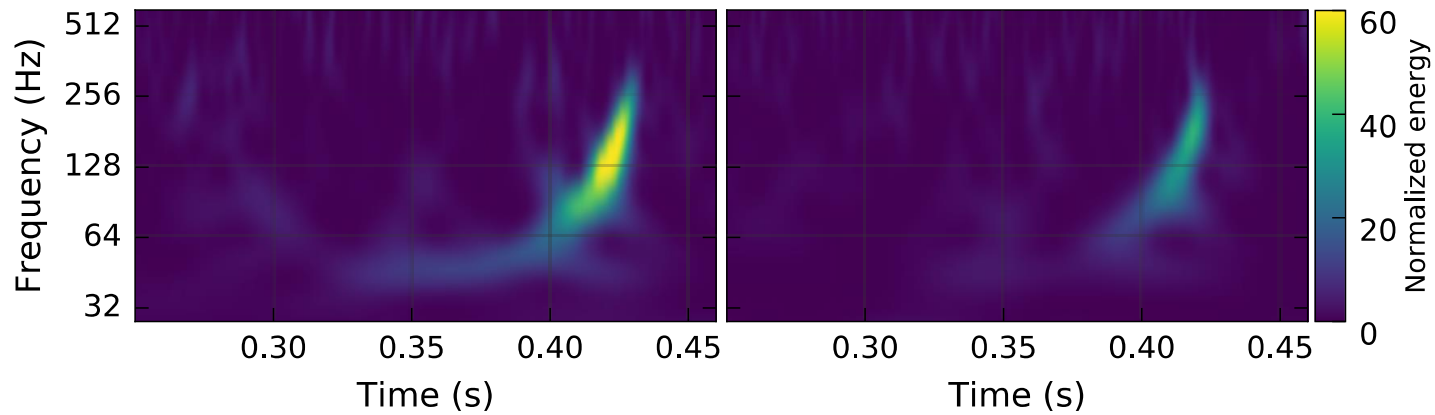
- The same waveform must be seen at the Louisiana and Washington sites within ± 10 msec
- The waveform at a site cannot be coincident with signals from the environmental monitors at the site
 - 3 axis seismometers
 - 3 axis accelerometers on the chambers
 - Tilt meters
 - Microphones
 - Magnetometers
 - RF monitors
 - Line voltage monitors
 - Wind speed monitors
- The waveform at a site cannot be coincident with auxiliary signals in the interferometer not directly associated with the gravitational wave output
 - Alignment control signals
 - Laser frequency and amplitude control signals
 - Approximately 10^5 sensing signals within the instrument

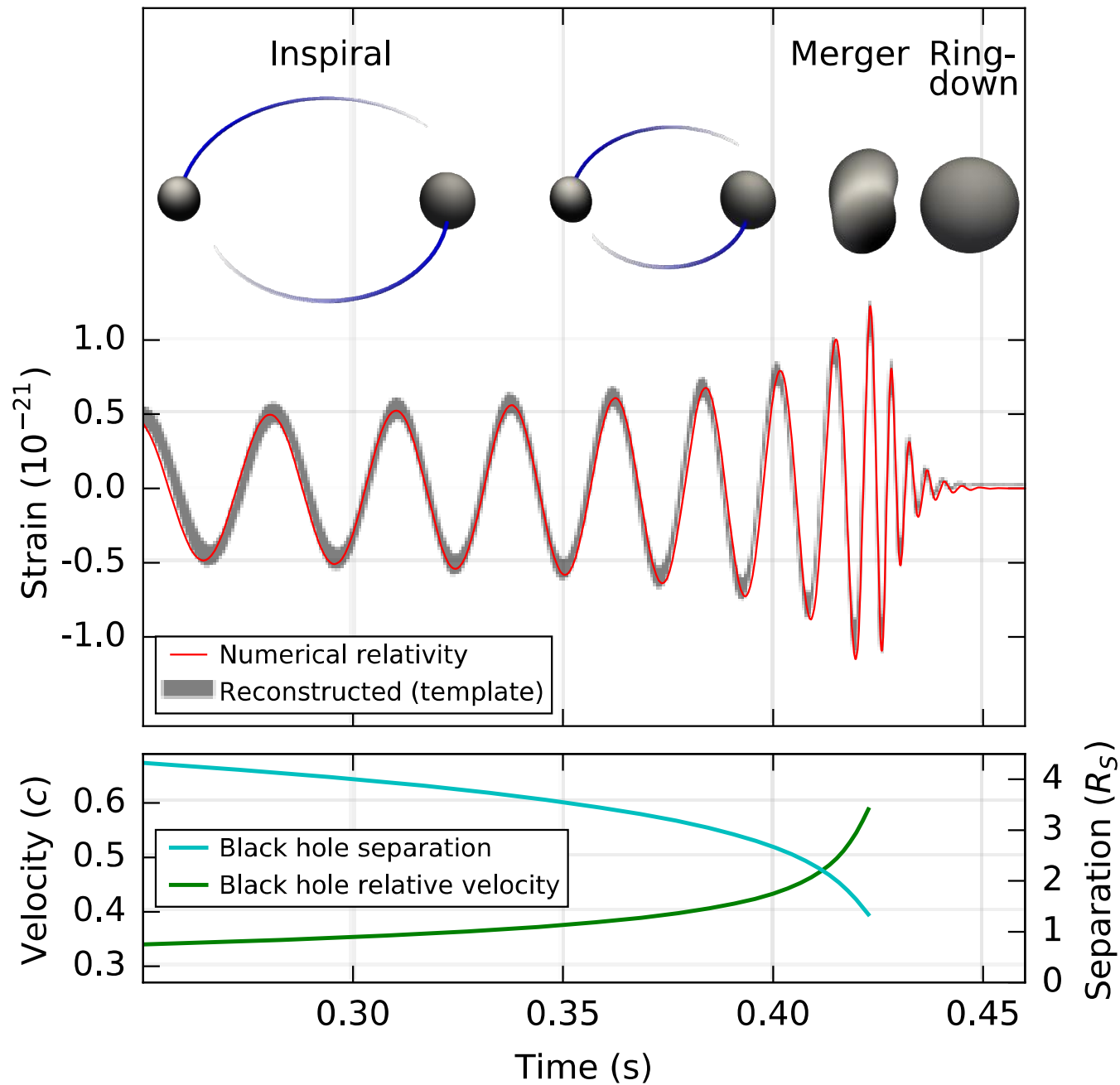
Hanford, Washington (H1)

Livingston, Louisiana (L1)

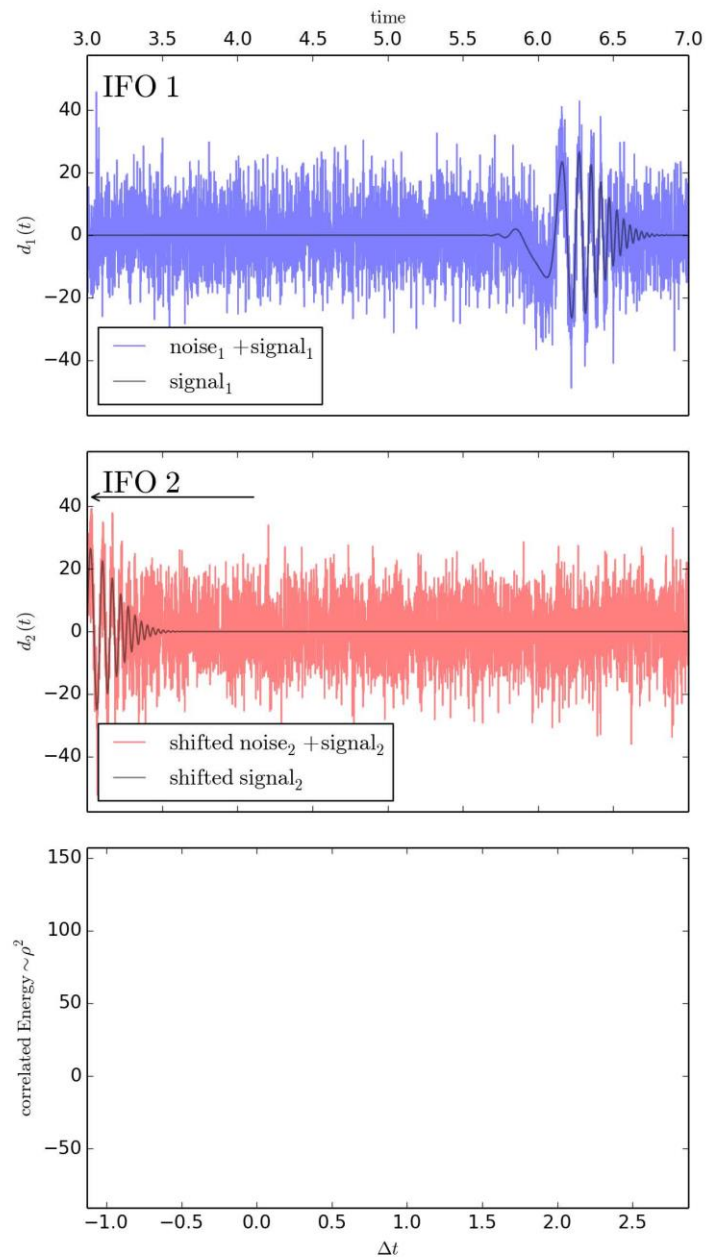
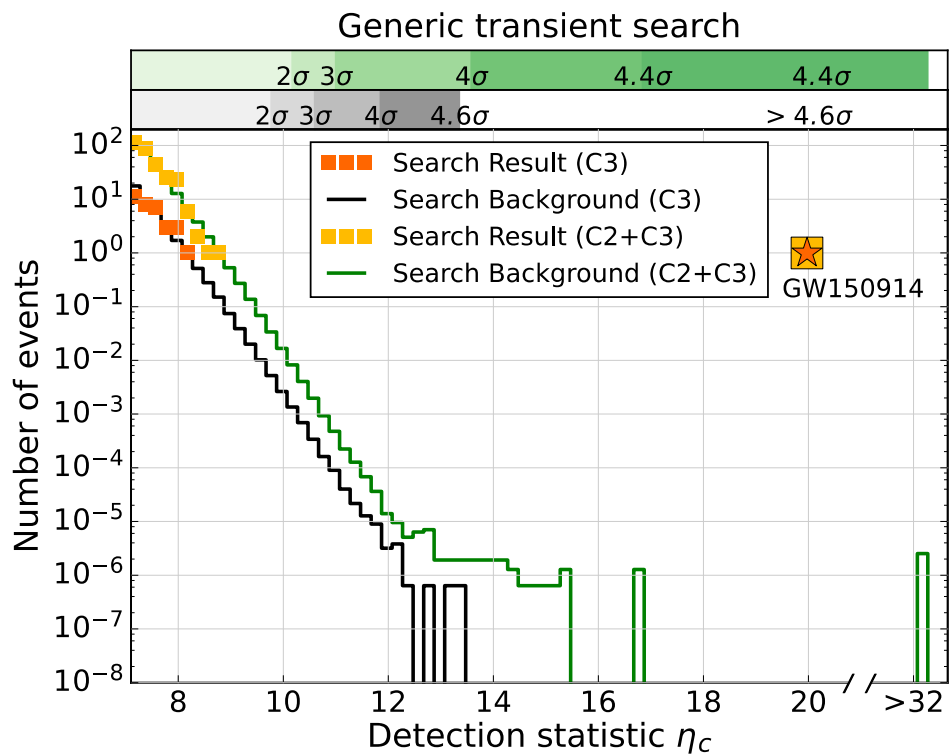


Simple high-low pass filter with notches

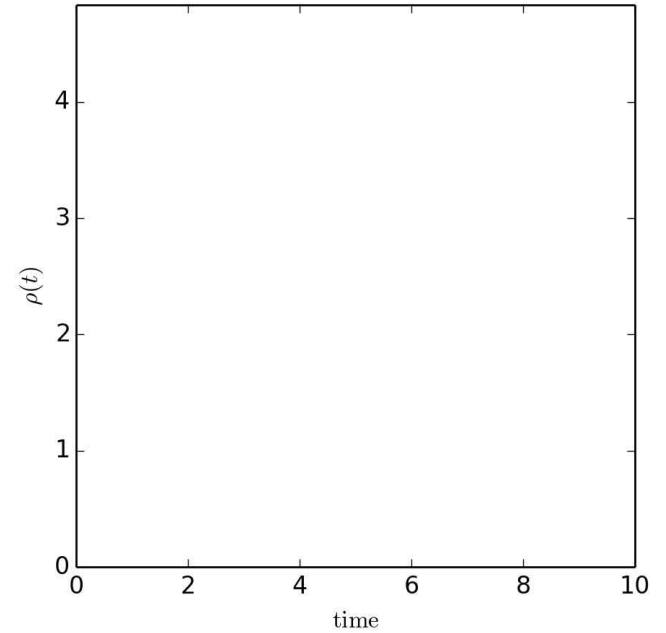
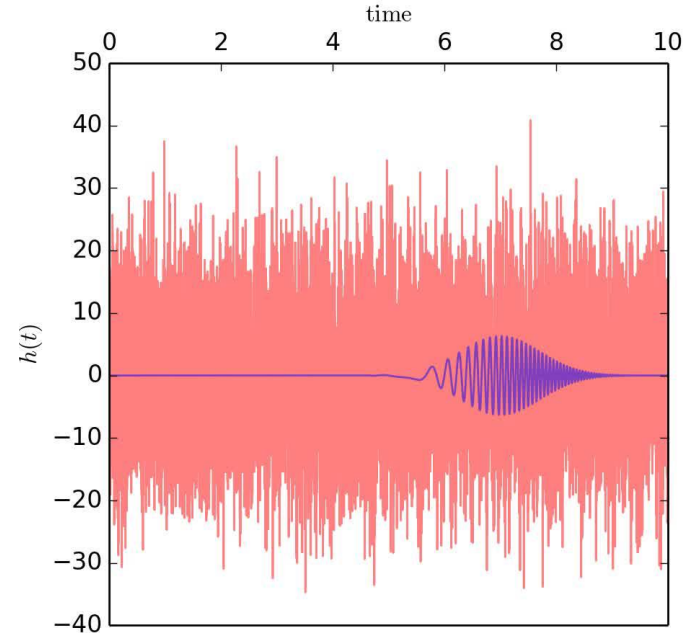
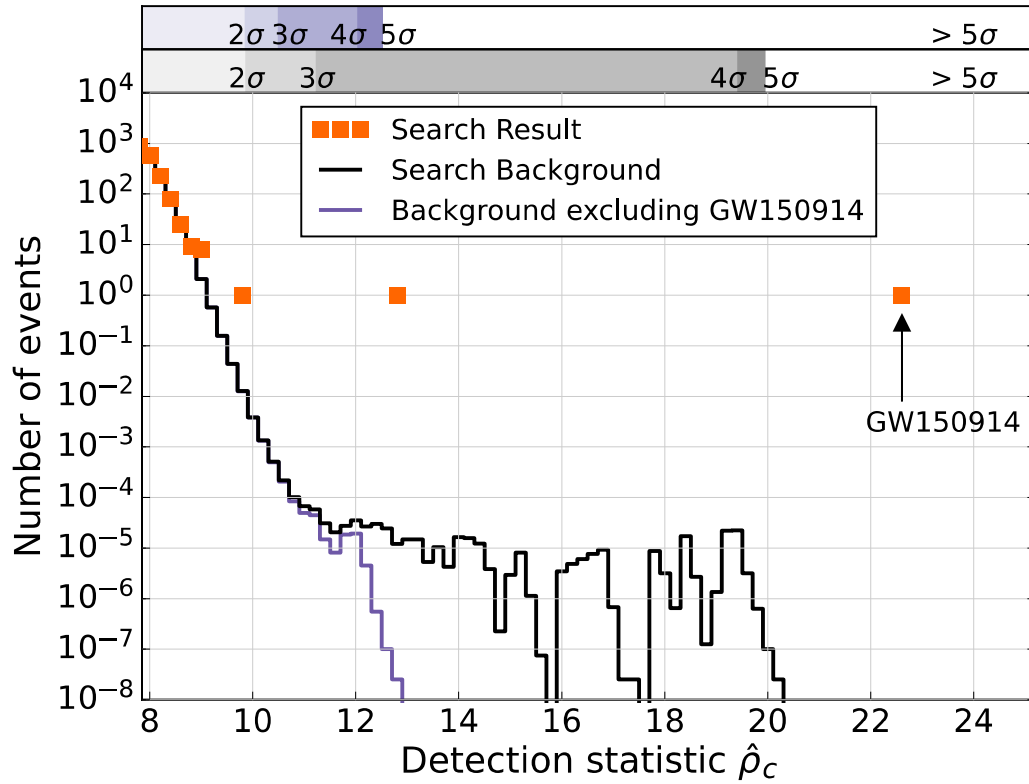




Generic transient search

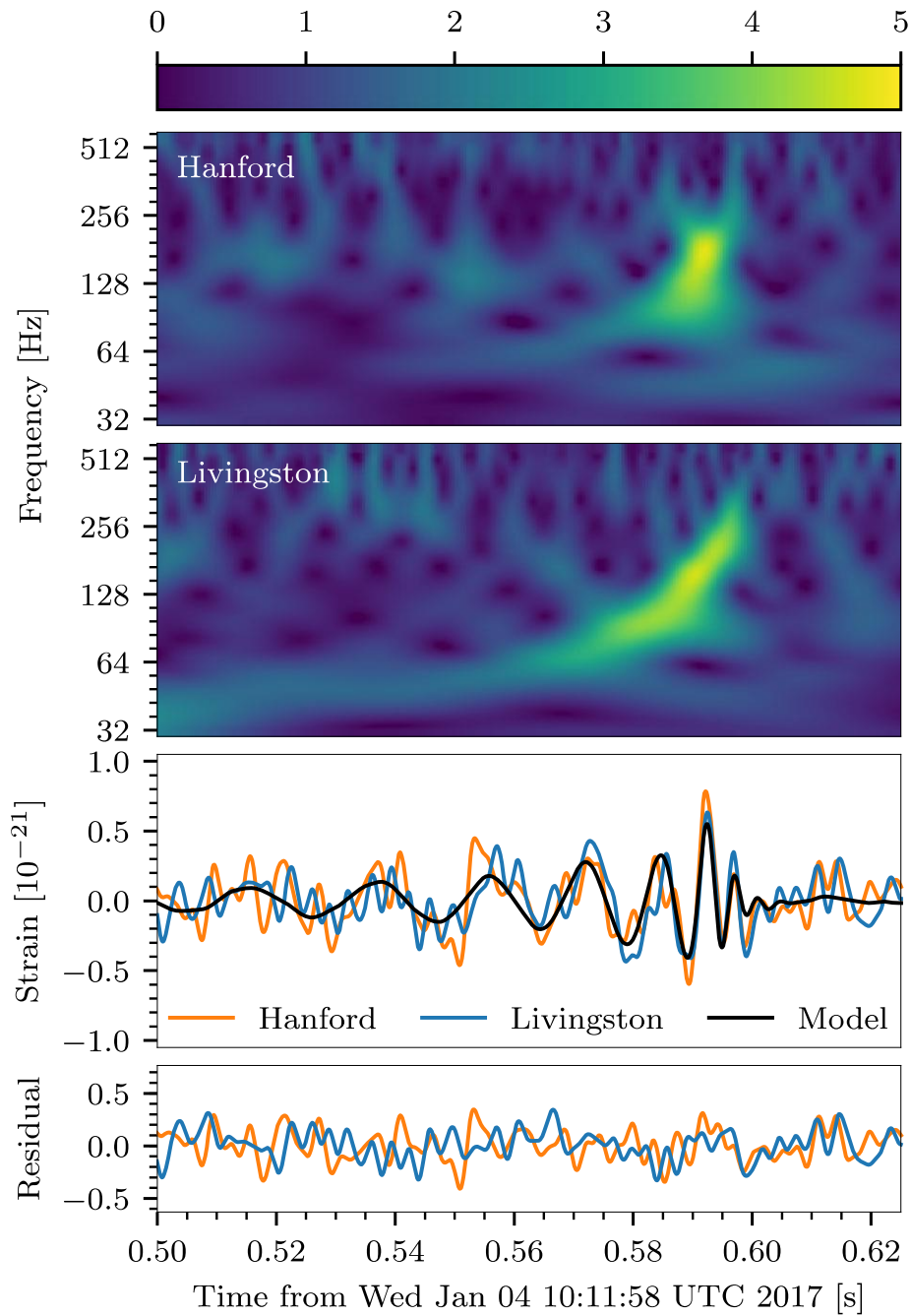


Modeled search followed by C^2 cut

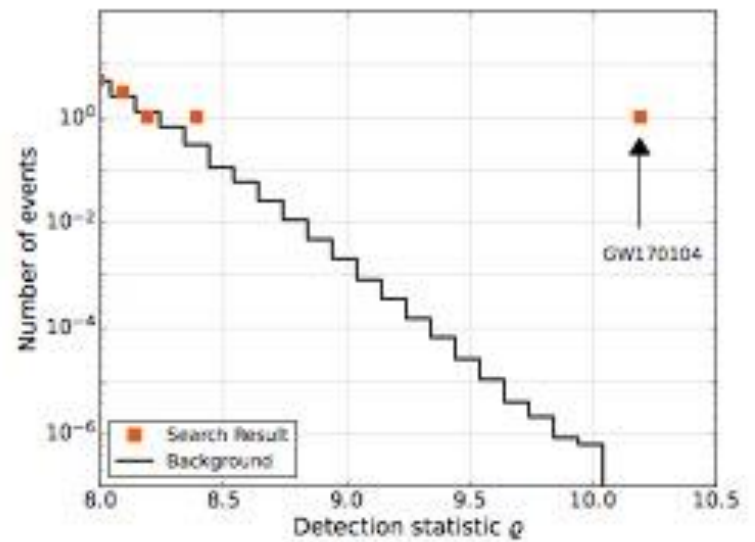


False alarm rate from time slides

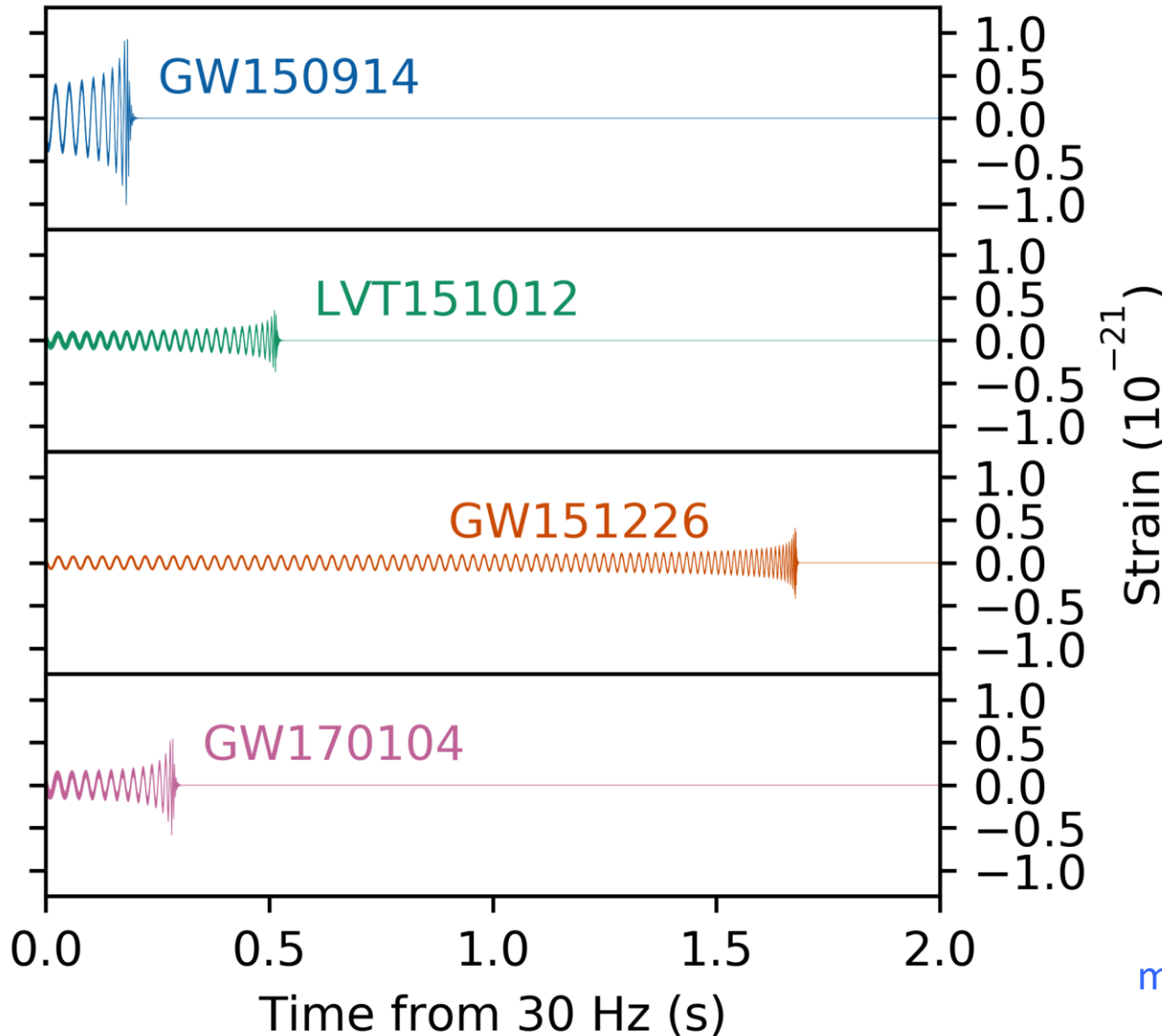
$$R = \frac{t_{\text{corr}}}{t_{\text{total}}^2} = \frac{1}{N_{\text{ind}} t_{\text{total}}}$$



GW 170104



Results of O1 and O2 run announced June 1, 2017



$m_1=36, m_2= 29, \Delta m=3$

if at 1 au

$h \sim 10^{-6}$

$I_g \sim 10^{25} \text{ w/m}^2$

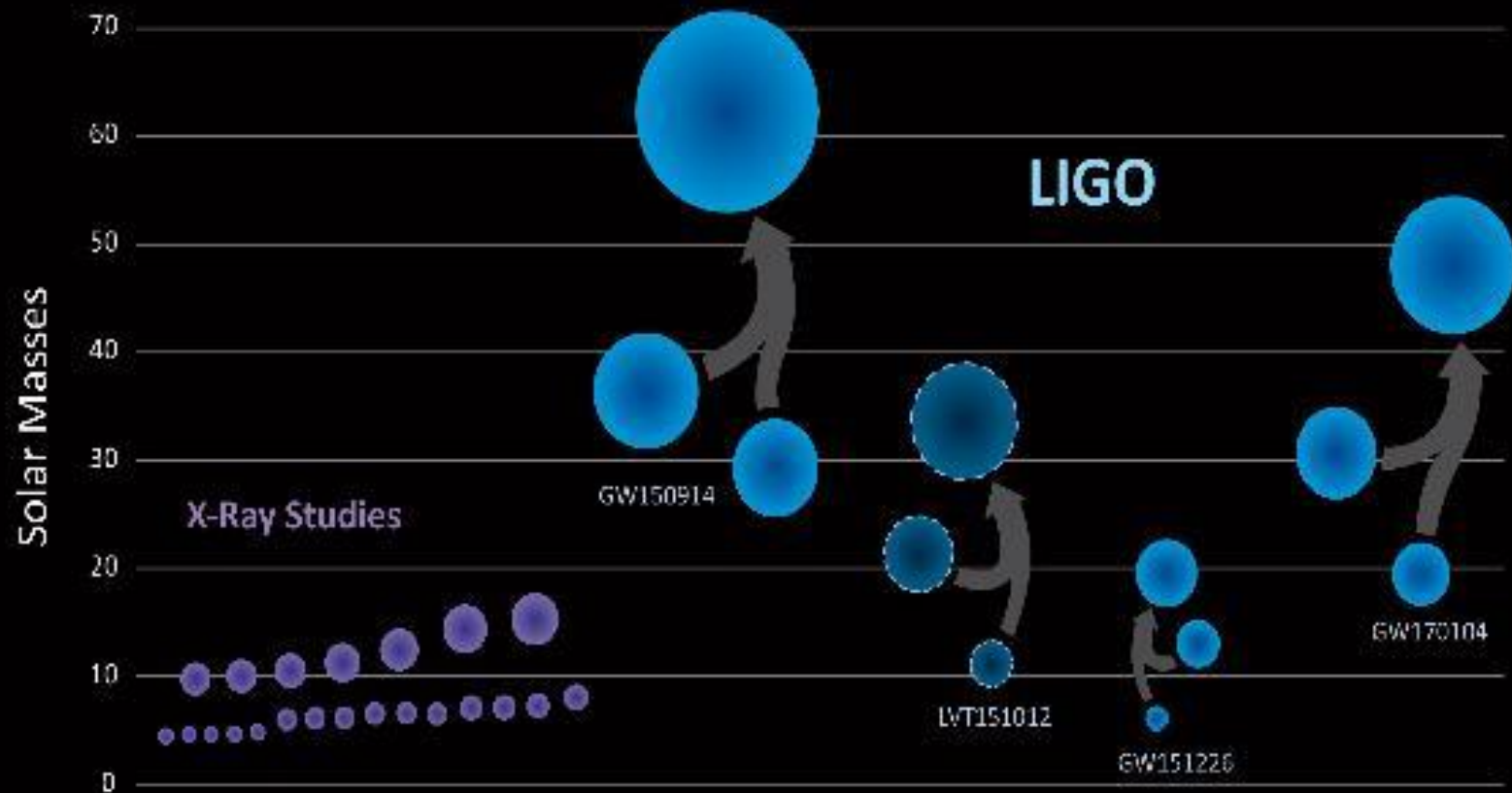
$m_1=23, m_2= 13, \Delta m=1.5$

$m_1=14.2, m_2= 7.5, \Delta m=1$

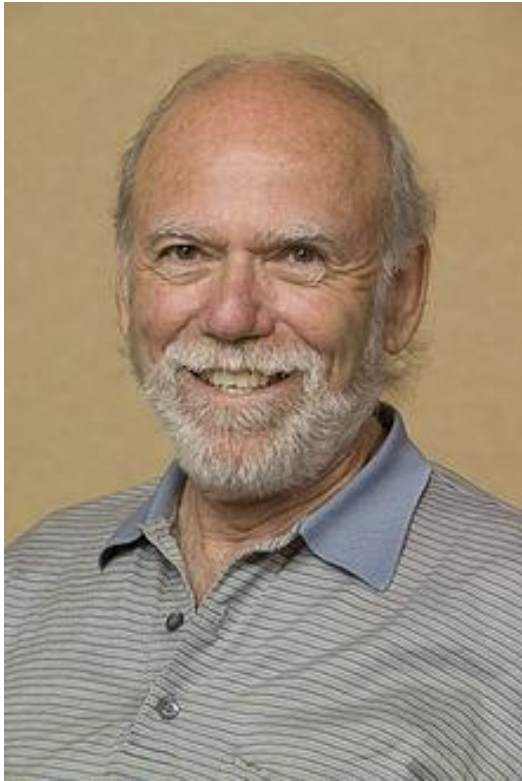
$m_1=31, m_2= 19, \Delta m=2$

masses in source frame

Black Holes of Known Mass



The real start 1994



B. Barish



G. Sanders



A. Lazzarini



S. Whitcomb



D. Coyne

LSC



P. Saulson
2nd Spokesperson



D. Reitze
3rd LSC Spokesperson
4th LIGO Director



G. Gonzalez
4th Spokesperson

LIGO Laboratory



J. Marx
3rd LIGO Director

Advanced LIGO Project



D. Coyne



D. Shoemaker



P. Fritschel



V. Frolov

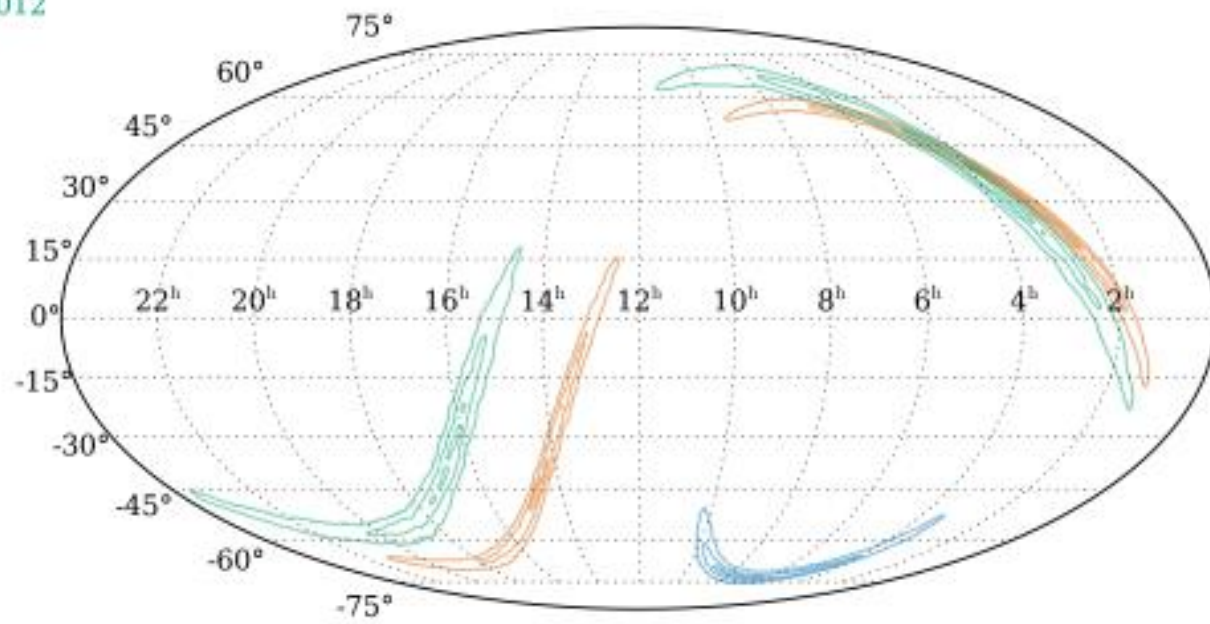


D. Sigg

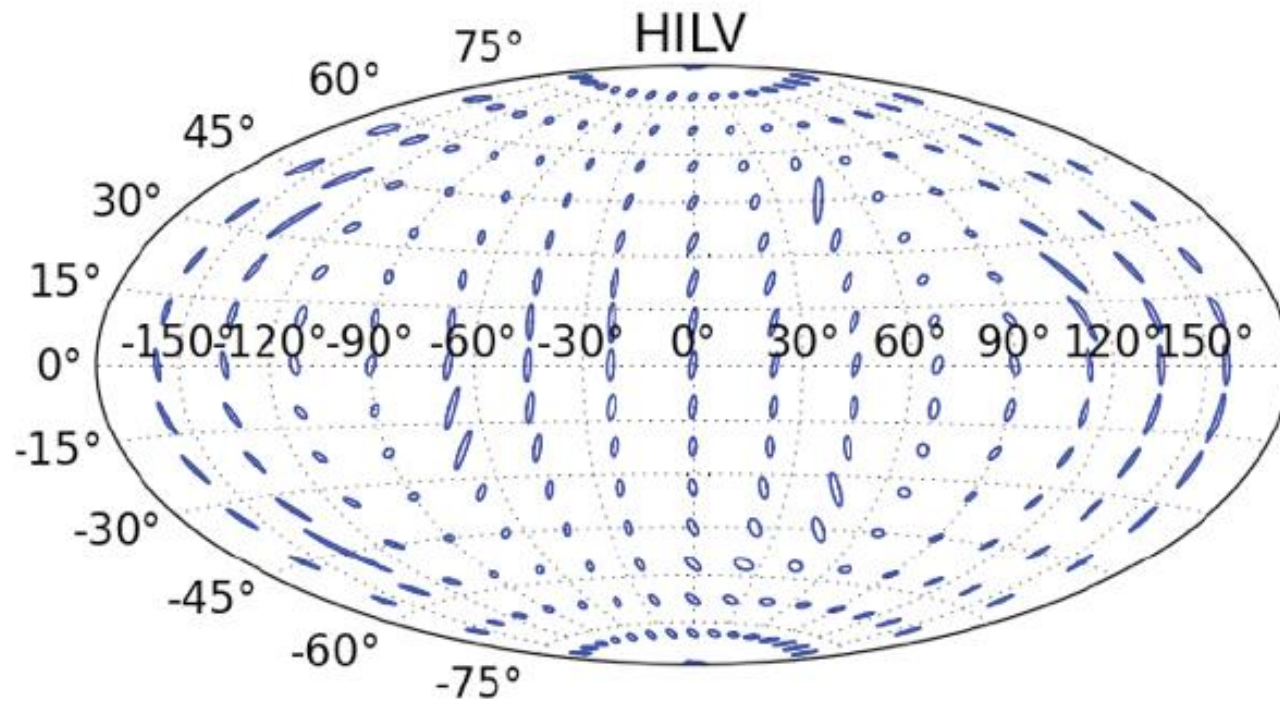
Classes of sources and searches

- **Compact binary inspiral: template search**
 - BH/BH
 - NS/NS and BH/NS
- **Low duty cycle transients: wavelets, T/f clusters**
 - Supernova
 - BH normal modes
 - Unknown types of sources
- **Triggered searches**
 - Gamma ray bursts
 - EM transients
- **Periodic CW sources**
 - Pulsars
 - Low mass x-ray binaries (quasi periodic)
- **Stochastic background**
 - Cosmological isotropic background
 - Foreground sources : gravitational wave radiometry

GW150914
GW151226
LVT151012



Localization with more detectors



Fairhurst 2011

age of universe

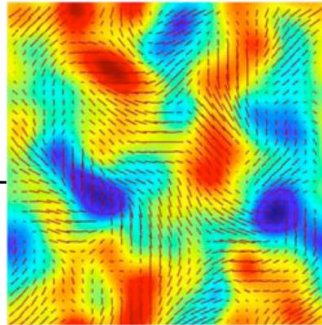
years

hours

minutes

1/10 to 1/1000 sec

*Cosmic Microwave Background
Polarization B Modes*



h

10^{-5}

10^{-10}

10^{-15}

10^{-20}

10^{-25}

Primeval gravitational waves from inflationary epoch

Measured at epoch of recombination $z \sim 1000$ and reionization $z \sim 6$

Pulsar Timing



Supermassive BH coalescences

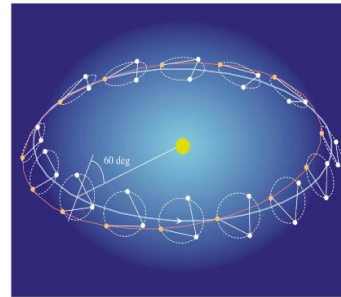
Isotropic GW background from unresolved sources

Massive BH coalescences

Small mass/BH infalls

White dwarf binaries in our galaxy

Space-based Interferometers



Compact binary coalescences: neutron stars and black holes

Asymmetric pulsar rotations

Ground-based Interferometers



Gravitational Wave Spectrum

10^{-16}

10^{-12}

10^{-8}

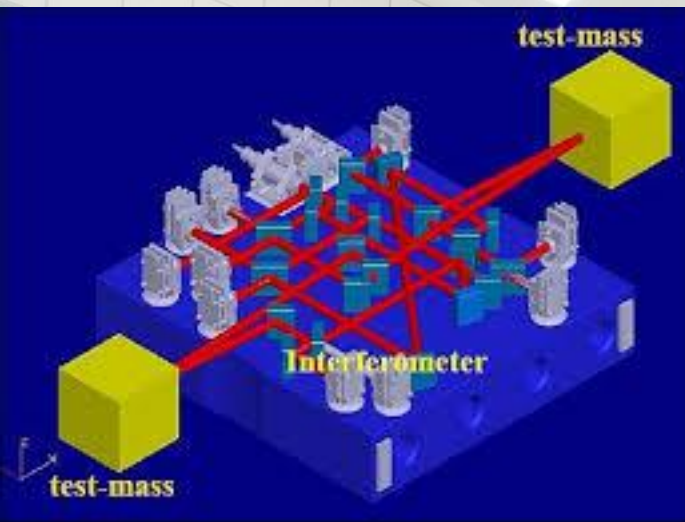
10^{-4}

10^0

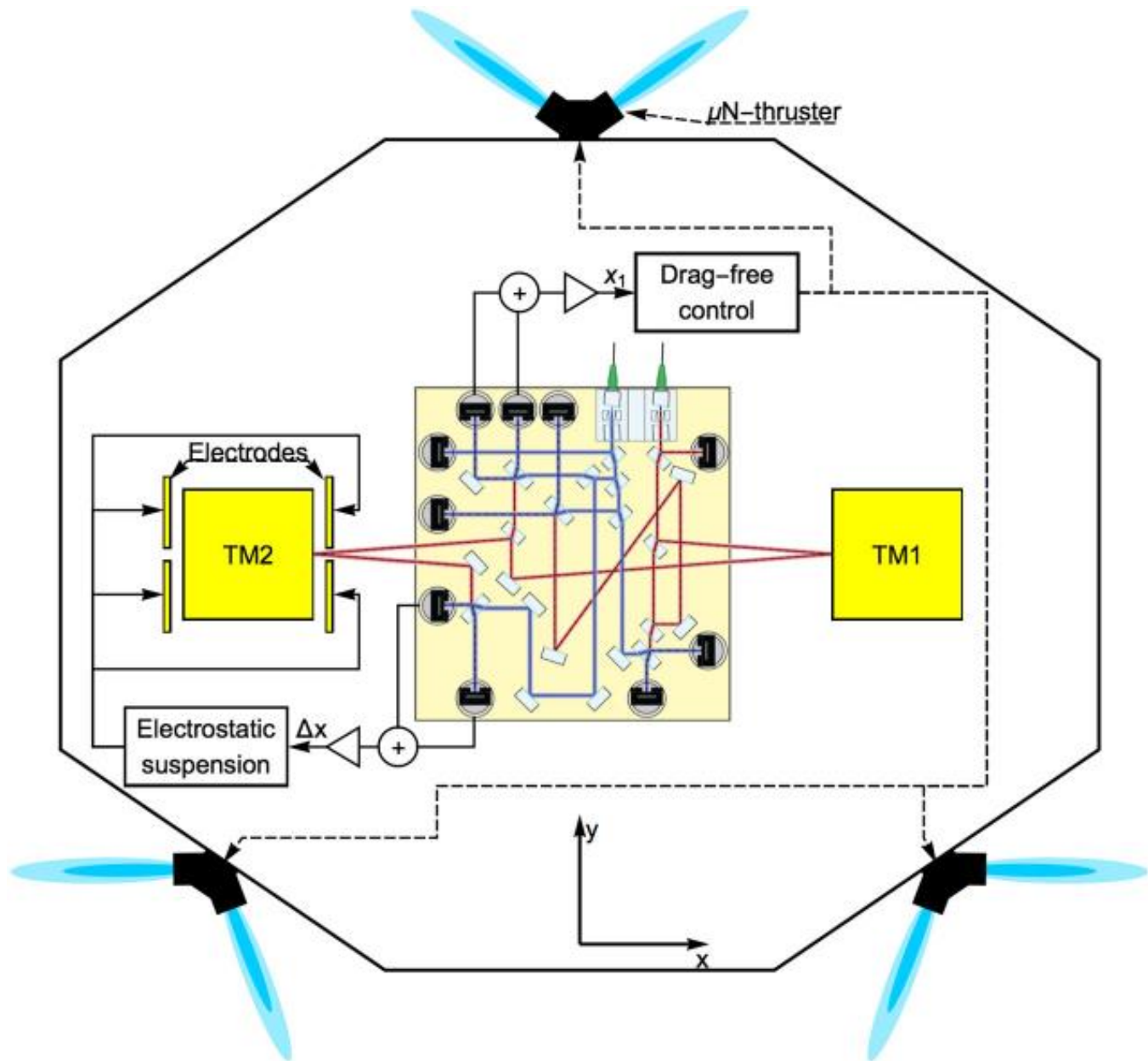
10^4

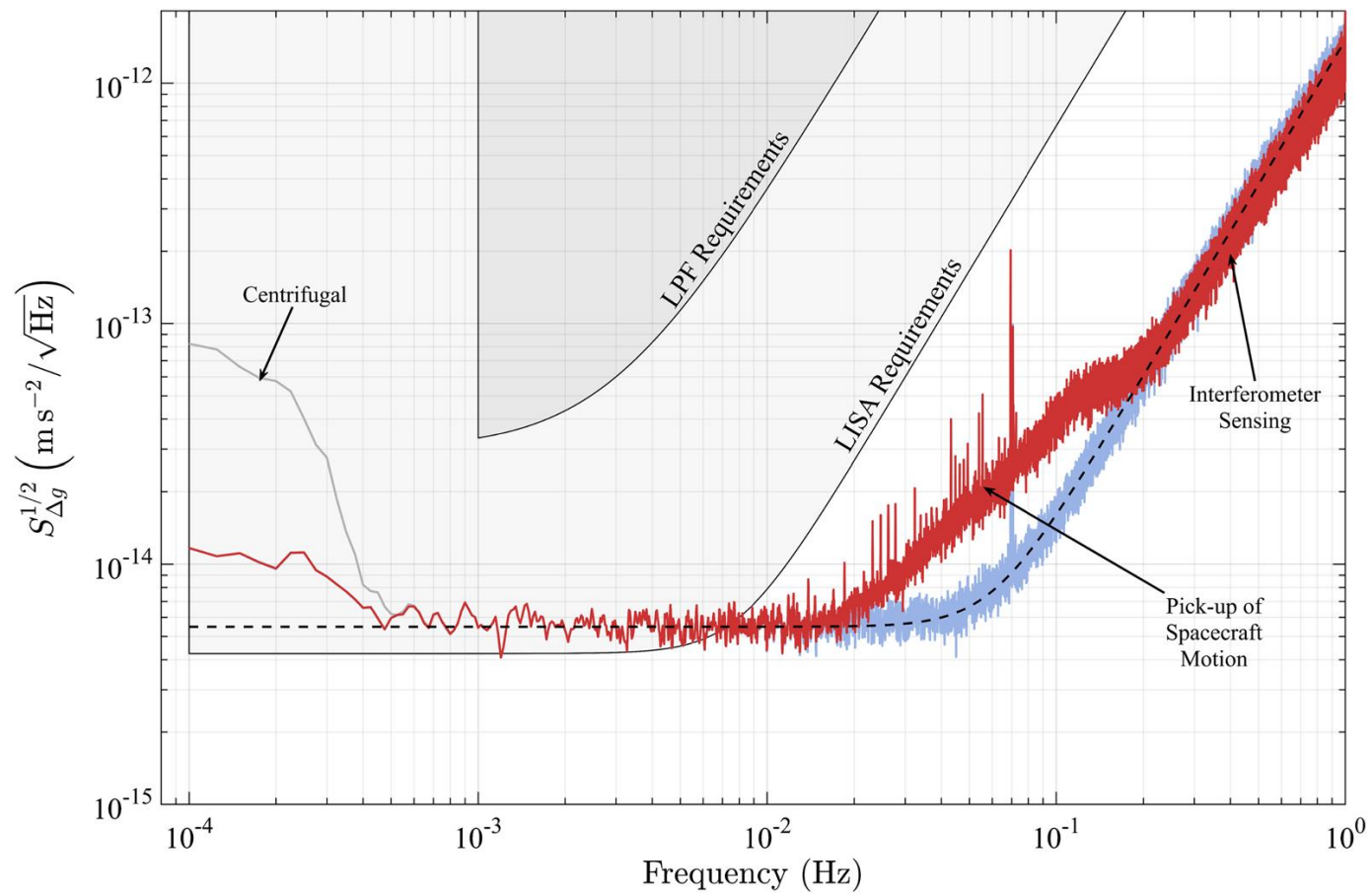
Frequency Hz

LISA Pathfinder



Launched 12/03/2015
At L1, masses released
Passed acceleration tests
Next. thruster tests





age of universe

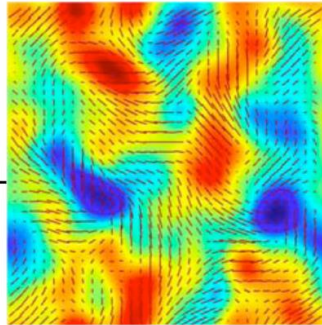
years

hours

minutes

1/10 to 1/1000 sec

*Cosmic Microwave Background
Polarization B Modes*



h

10^{-5}

10^{-10}

10^{-15}

10^{-20}

10^{-25}

Primeval gravitational waves from inflationary epoch

Measured at epoch of recombination $z \sim 1000$ and reionization $z \sim 6$

Pulsar Timing



Supermassive BH coalescences

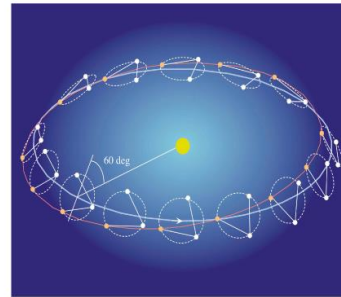
Isotropic GW background from unresolved sources

Massive BH coalescences

Small mass/BH infalls

White dwarf binaries in our galaxy

Space-based Interferometers



Compact binary coalescences: neutron stars and black holes

Asymmetric pulsar rotations

Ground-based Interferometers



Gravitational Wave Spectrum

10^{-16}

10^{-12}

10^{-8}

10^{-4}

10^0

10^4

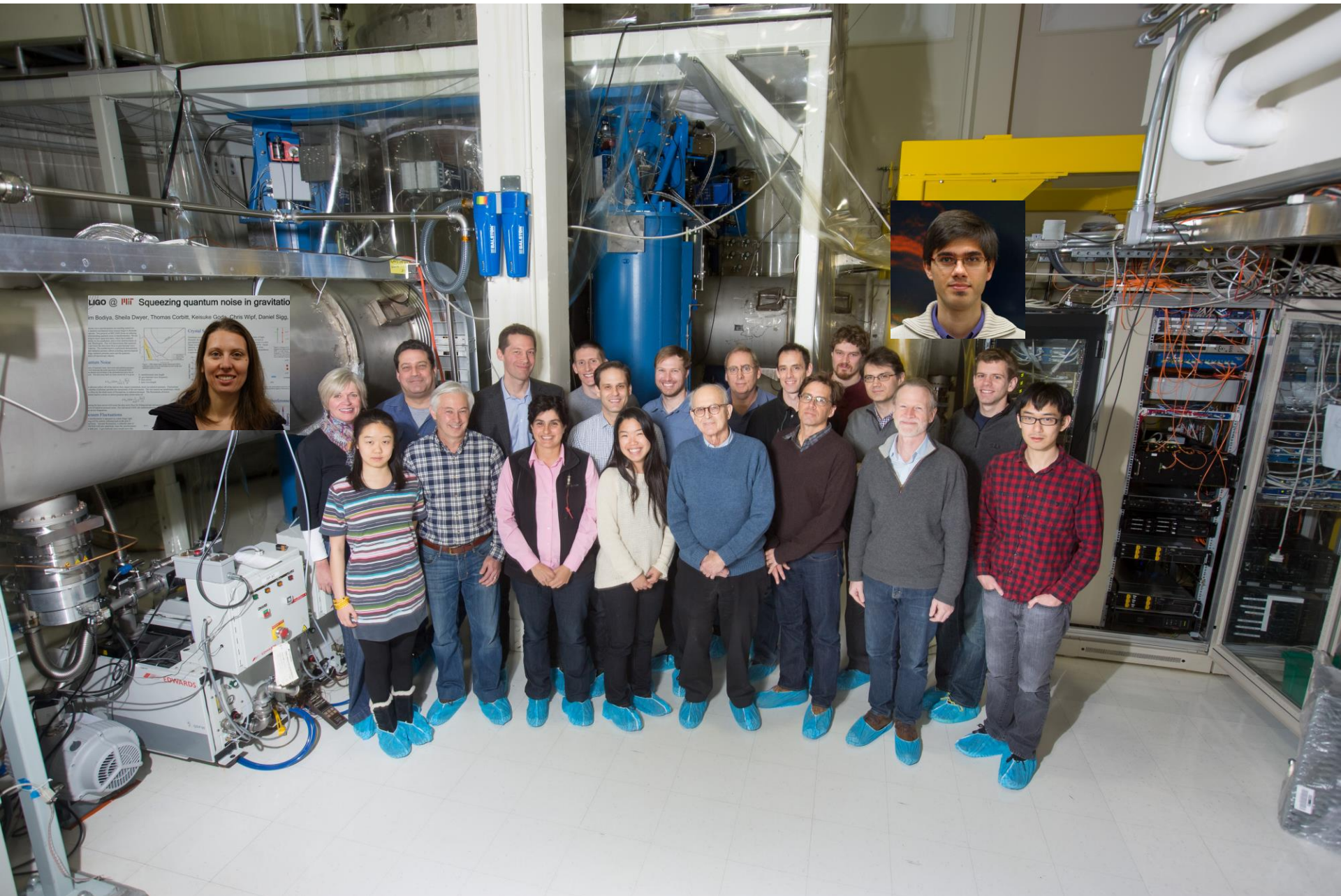
Frequency Hz



LIGO HANFORD OBSERVATORY STAFF



LIGO LIVINGSTON OBSERVATORY STAFF



MIT LIGO LABORATORY GROUP



CALTECH LIGO LABORATORY GROUP

Spare slides follow

After Feb 11, 2016

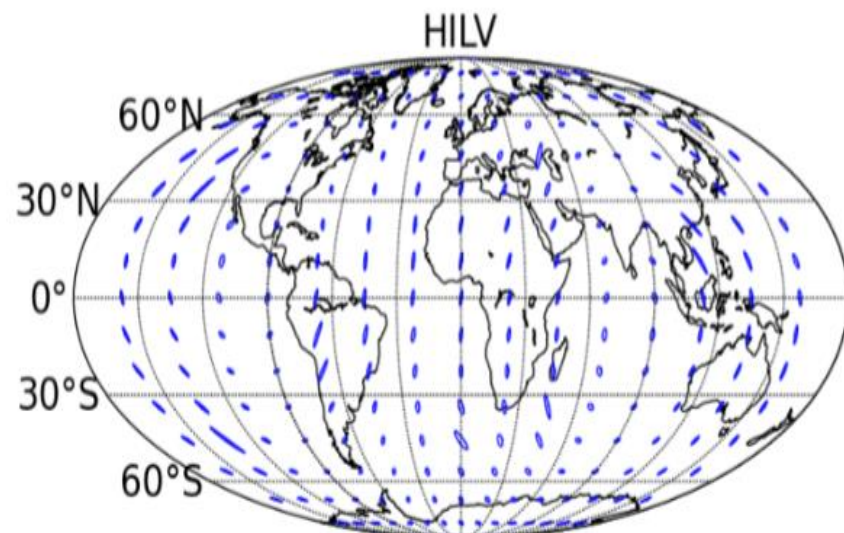
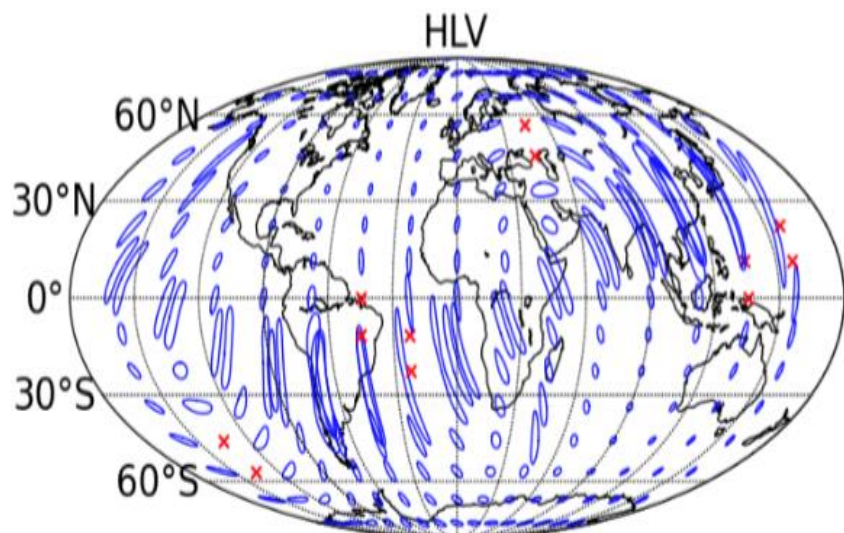
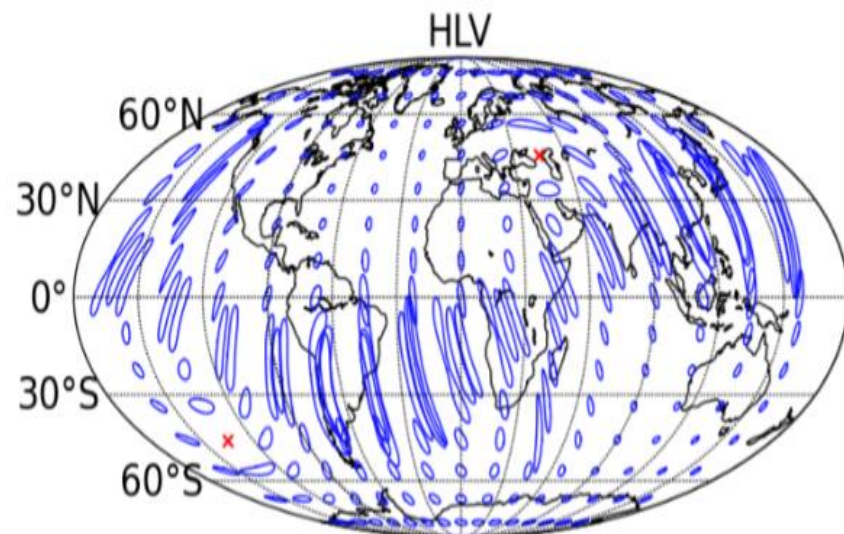
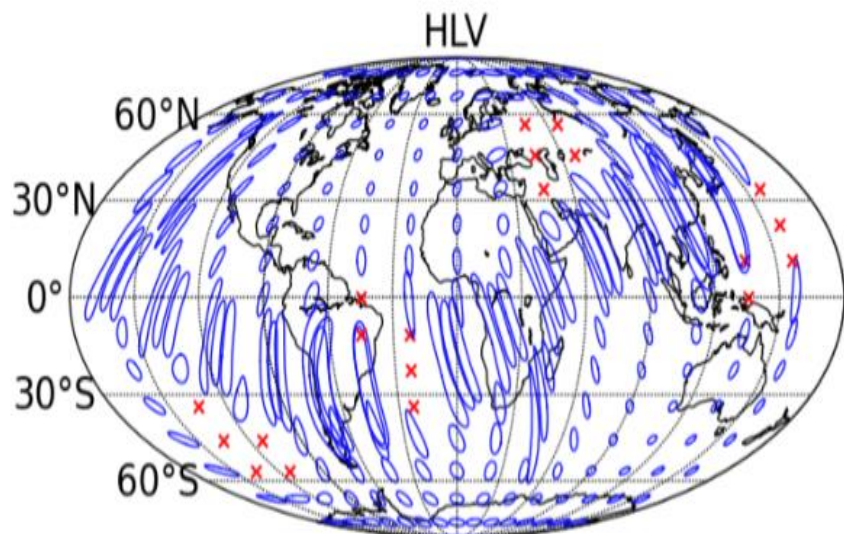


Matt Weber

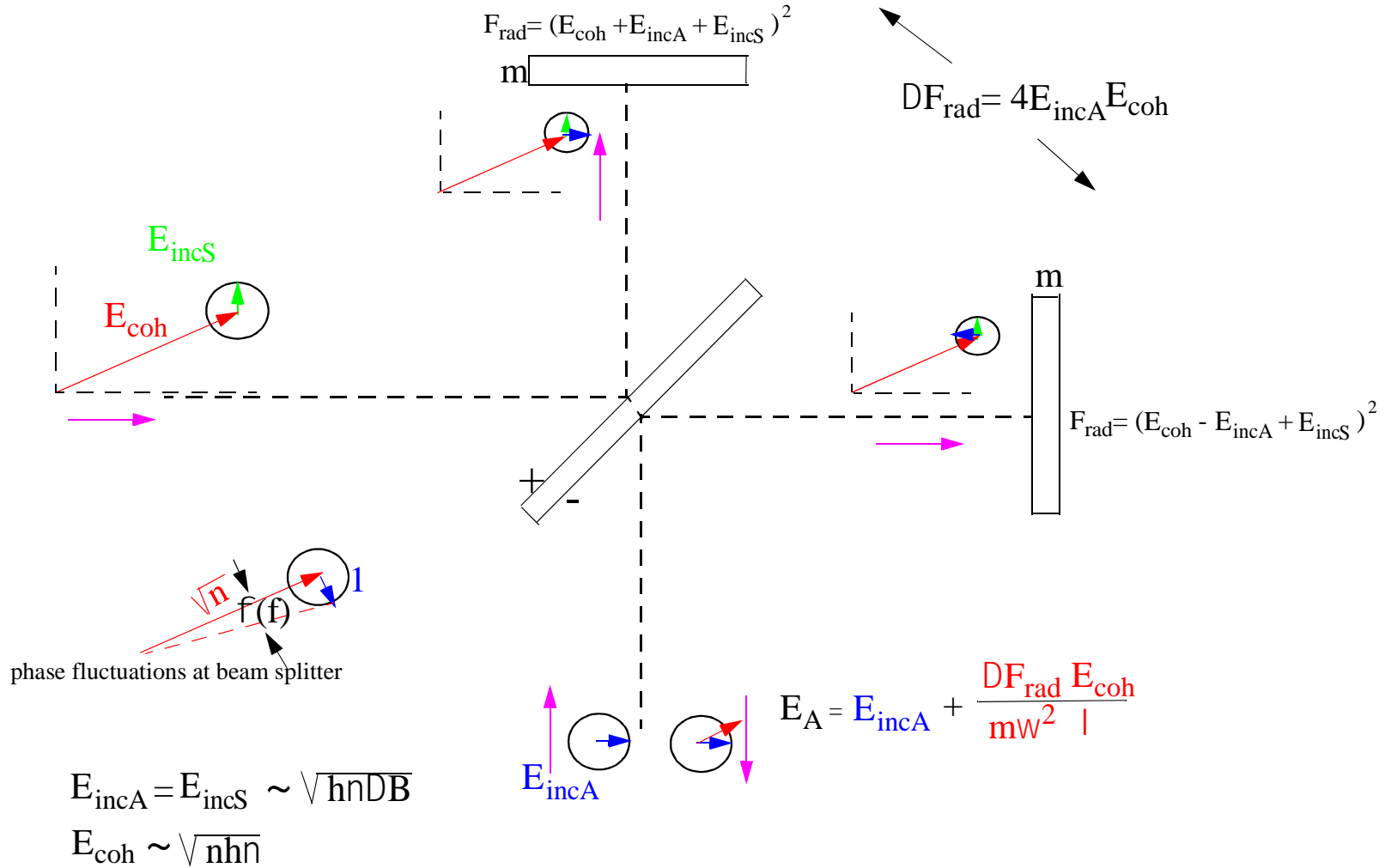


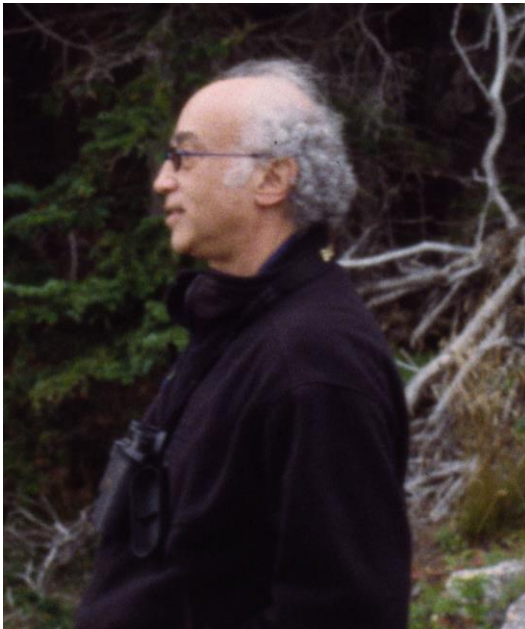
*“Was that you I heard just now,
or was it two black holes colliding*

New Yorker Feb 12,, 2016



Quantum Noise in the Michelson Interferometer





R. Isaacson (Gravitational Physics NSF)

Gravitational Radiation in the Limit of High Frequency. II. Nonlinear Terms and the Effective Stress Tensor*

RICHARD A. ISAACSON†

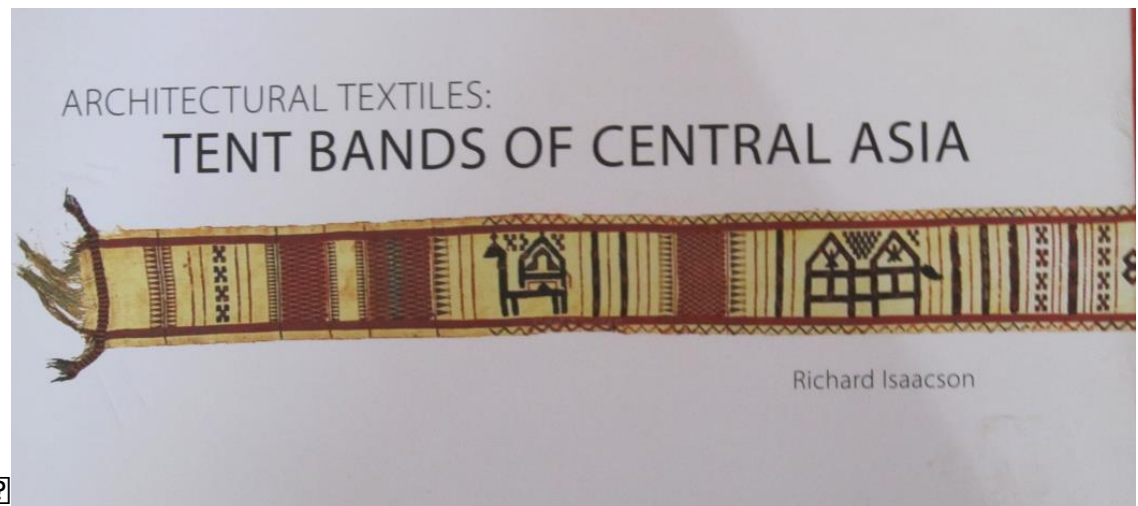
Department of Physics and Astronomy, University of Maryland, College Park, Maryland

(Received 14 July 1967)

The high-frequency expansion of a vacuum gravitational field in powers of its small wavelength is continued. We go beyond the previously discussed linearization of the field equations to consider the lowest-order nonlinearities. These are shown to provide a natural, gauge-invariant, averaged stress tensor for the effective energy localized in the high-frequency gravitational waves. Under the assumption of the WKB form for the field, this stress tensor is found to have the same algebraic structure as that for an electromagnetic null field. A Poynting vector is used to investigate the flow of energy and momentum by gravitational waves, and it is seen that high-frequency waves propagate along null hypersurfaces and are not back-scattered by the lowest-order nonlinearities. Expressions for the total energy and momentum carried by the field to flat null infinity are given in terms of coordinate-independent hypersurface integrals valid within regions of high field strength. The formalism is applied to the case of spherical gravitational waves where a news function is obtained and where the source is found to lose exactly the energy and momentum contained in the radiation field. Second-order terms in the metric are found to be finite and free of divergences of the $(\ln r)/r$ variety.



M. Bardon (Director of Physics NSF)



Plane gravitational waves

Transverse Plane Wave Solutions with “Electric”
and “Magnetic” Terms

Geometric Interpretation

$$ds^2 = g_{ij} dx^i dx^j$$

$$g_{ij} = \eta_{ij} + h_{ij} \quad \text{weak field}$$

$$\eta_{ij} = \begin{pmatrix} 1 & & & 0 \\ & -1 & & \\ 0 & & -1 & \\ & & & -1 \end{pmatrix} \quad \begin{array}{l} \text{Minkowski Metric of} \\ \text{Special Relativity} \end{array}$$

Gravity Wave Propagating in the x_1 Direction

$$h_{ij} = \begin{pmatrix} 0 & 0 & 0 & 0 \\ 0 & 0 & 0 & 0 \\ 0 & 0 & h_{22} & h_{23} \\ 0 & 0 & h_{32} & h_{33} \end{pmatrix} \quad \text{all } h_{ij} \ll 1$$

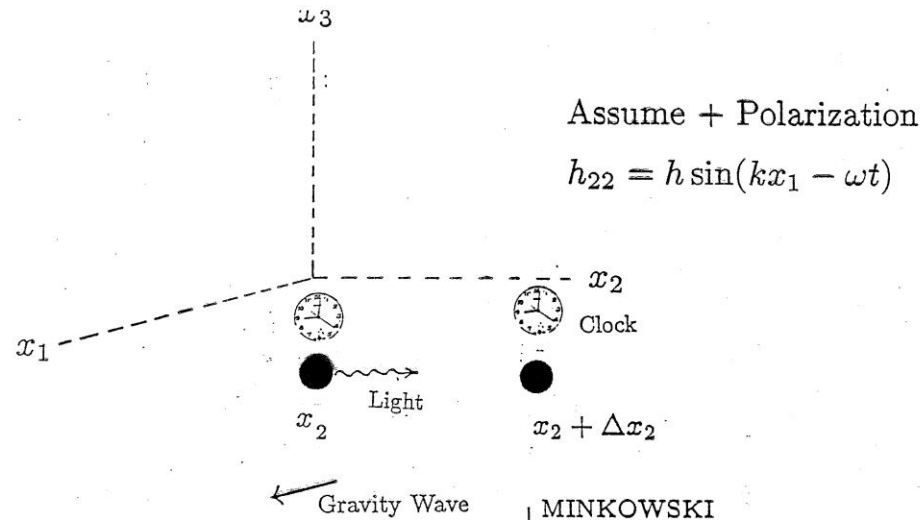
Plane Wave

$$\mathbf{h}_{22} = -\mathbf{h}_{33} \quad \mathbf{h}_{23} = \mathbf{h}_{32}$$

+ polarization × polarization

And All Only Function of $x_1 - ct$

Timing light in the gravitational wave



$$\Delta s^2 = 0 = c^2 \Delta t^2 - \left(1 + h \sin(kx_1 - \omega t)\right) \Delta x_2^2$$

LIGHT RAY

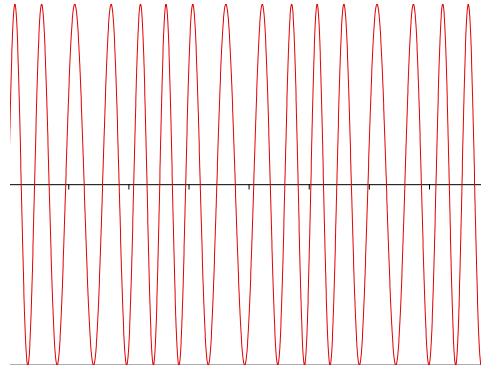
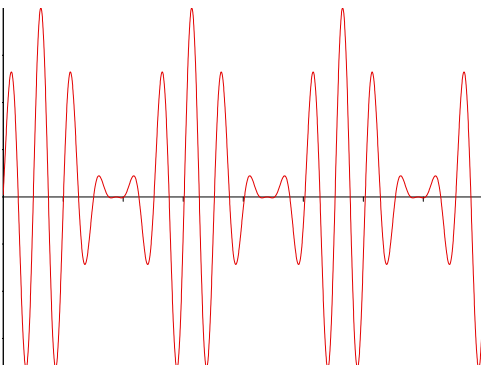
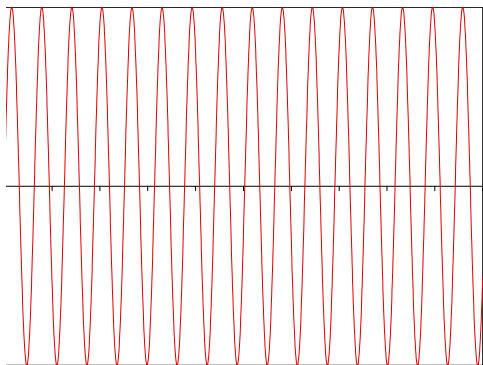
Let $\Delta t \ll \frac{1}{\omega}$ $h \ll 1$

$$c \Delta t \cong \left(1 + \frac{h}{2} \sin(kx_1 - \omega t)\right) \Delta x_2$$

←
 INFERRED
 DISTANCE
 BETWEEN POINTS

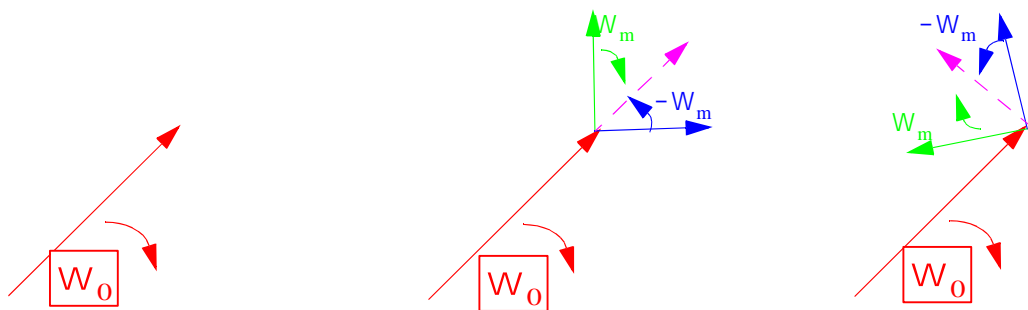
$$\frac{\delta(c \Delta t)}{\Delta x_2} = \frac{h}{2} \sin(kx_1 - \omega t) \quad \text{Time Dependent Strain}$$

$$\frac{\Delta l}{l} = \frac{h}{2} \quad \text{The Measurable Quantity}$$

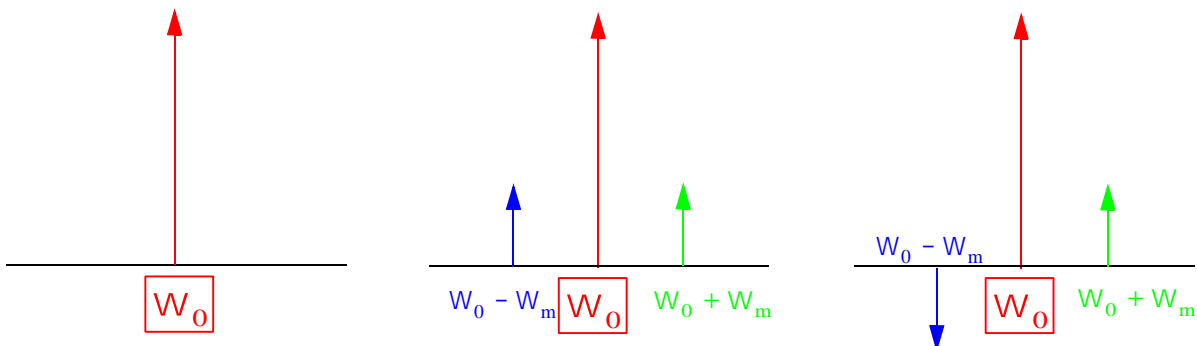


waveforms

phasors



spectrum



modulation

amplitude

phase

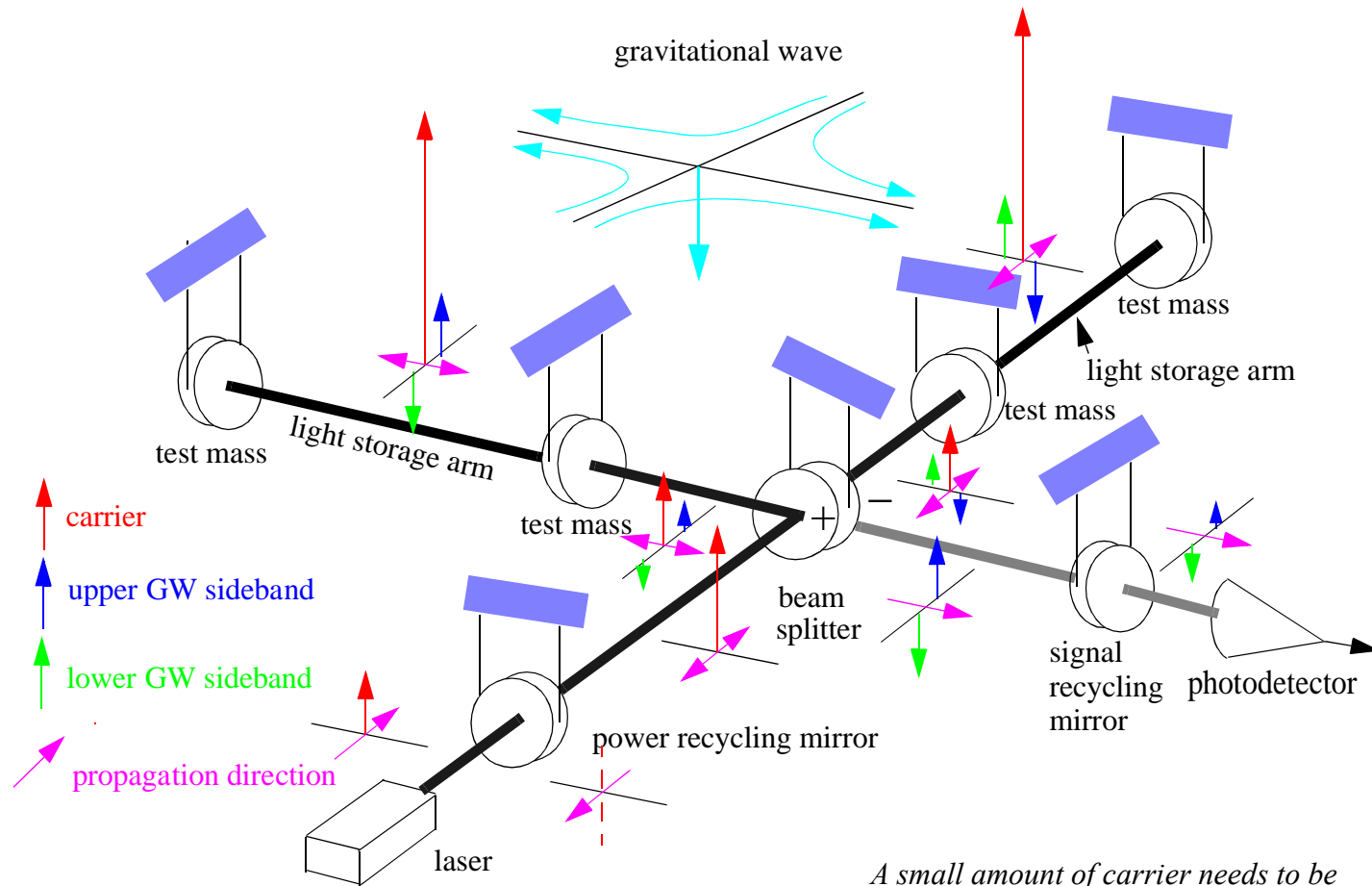
$$E(t) = \text{Re}(e^{iW_0 t})$$

$$\text{Re}(e^{iW_0 t} [1 + G(e^{-iW_m t} + e^{iW_m t})])$$

$$\text{Re}(e^{iW_0 t} [1 + G(e^{-iW_m t} - e^{iW_m t})])$$

MODULATION: Amplitude and Phase

Advanced LIGO Fabry-Perot Michelson Interferometer with GW sidebands



A small amount of carrier needs to be leaked to the photodetector to make the GW sidebands detectable

PENDULUM THERMAL NOISE

Pendulum Brownian motion

Dissipation leads to fluctuations

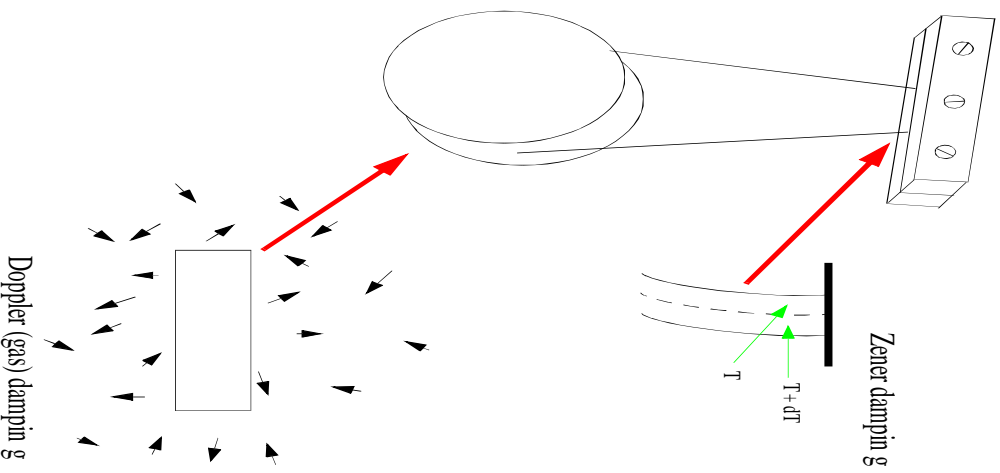
T_c = coherence or damping time

= Q x period of oscillator

Exchange with surroundings:

$$E(\text{thermal}) = \frac{kT}{T_c} t$$

Large $T_c \Rightarrow$ smaller fluctuations



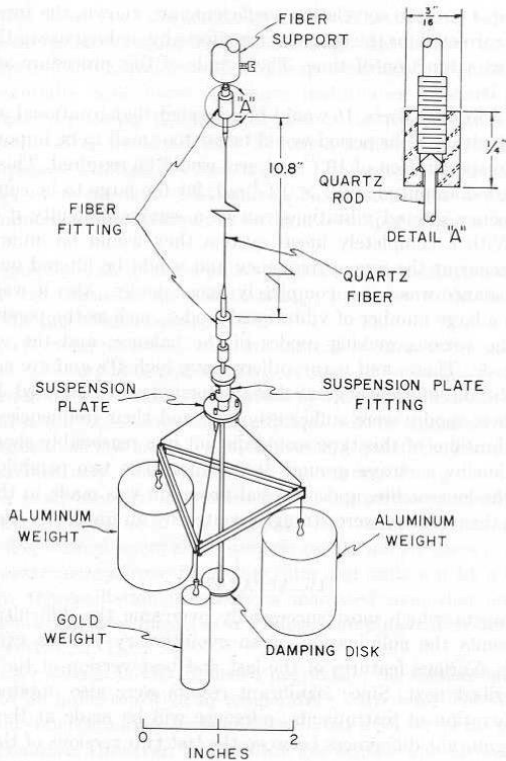


FIG. 3. The torsion balance suspension. The construction of both upper and lower fiber fittings is illustrated in Detail "A."



P.G. Roll, R. Krotkov, R.H. Dicke
 Principle of Equivalence Experiment

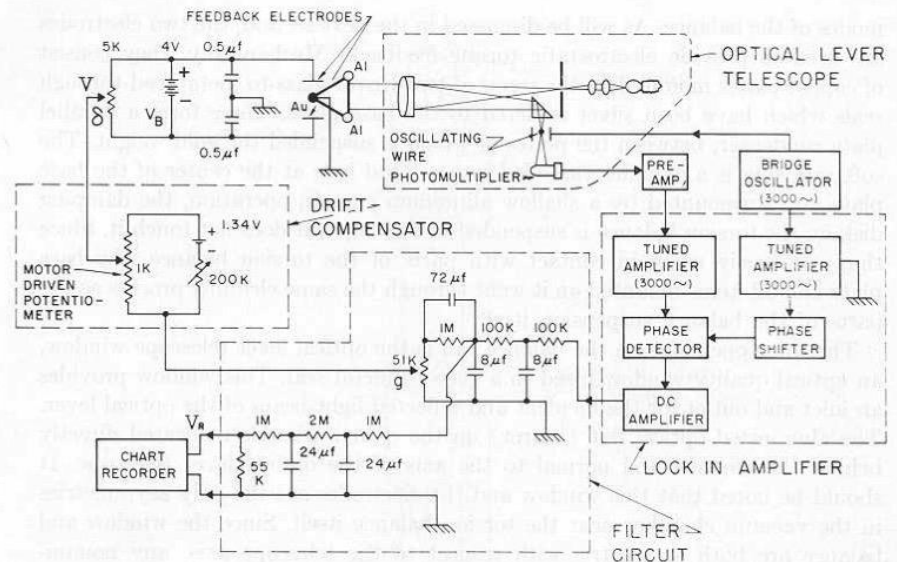
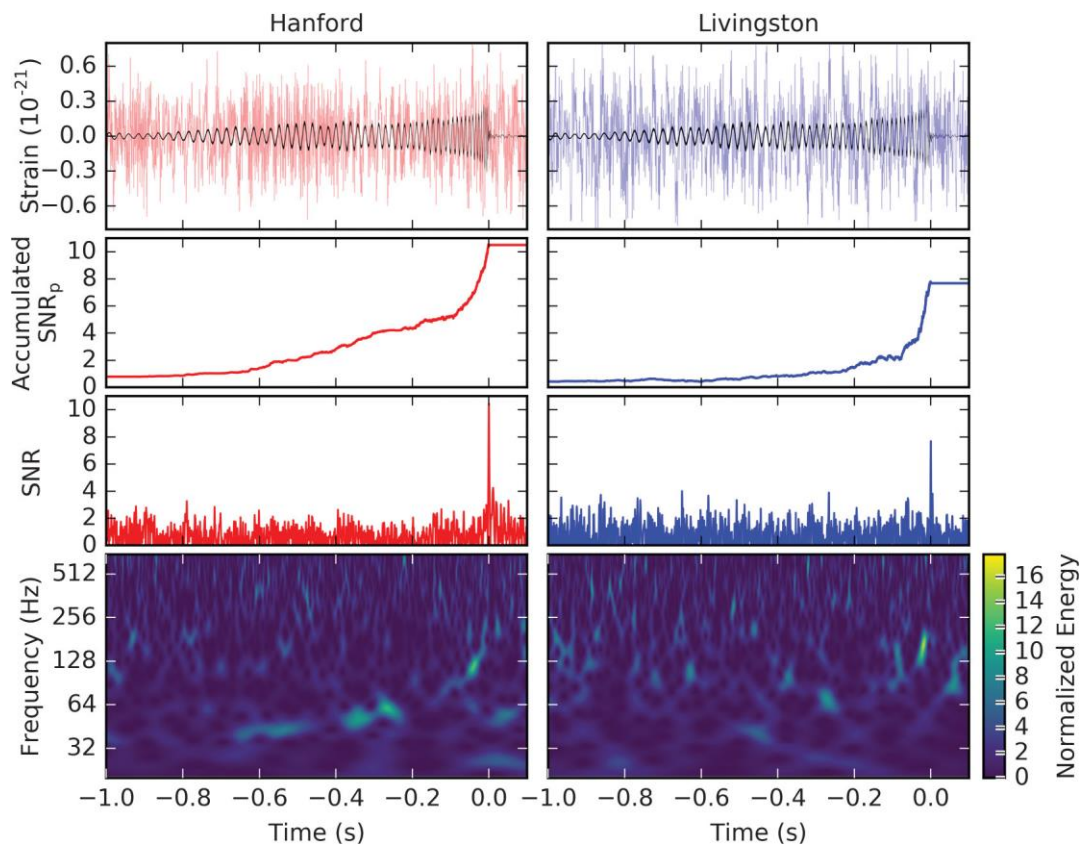
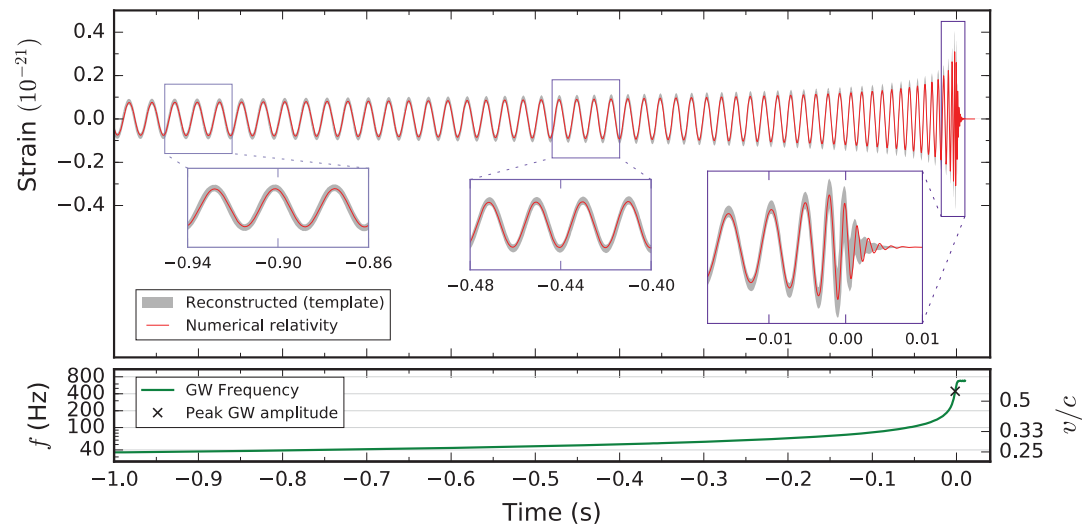


FIG. 6. Block diagram of the optical lever detection system

Servo cooling of a mechanical system





What is needed

Requirements:

$$h = \frac{DL}{L} < 10^{-22} \quad h(f) < 10^{-23} \text{ strain} / \sqrt{\text{Hz}} @ 100\text{Hz}$$

$$x < 10^{-18} \text{ meters} \quad x(f) < 10^{-19} \text{ meters} / \sqrt{\text{Hz}} @ 100\text{Hz}$$

What stands in the way:

Sensing the displacement

Quantum phase fluctuations: shot noise

Scattering at surfaces and gas

Optical distortion and loss

Laser amplitude and frequency noise

$$j(f) < 10^{-12} \text{ radians} / \sqrt{\text{Hz}} @ 100\text{Hz} \quad l = 1\text{m}$$

Believing that GW are causing the displacement

Seismic vibrations

Thermal fluctuations: suspensions and mirror surfaces

Quantum amplitude fluctuations: radiation pressure

Newtonian gravitational force fluctuations: $f < 20 \text{ Hz}$

$$F(f) < 10^{-12} \text{ newtons} / \sqrt{\text{Hz}} @ 100 \text{ Hz}$$

FRINGE SENSING

wavelength 1×10^{-6} m

$$h = \frac{\lambda}{L} \sim \frac{1}{Lb \sqrt{Nt}}$$

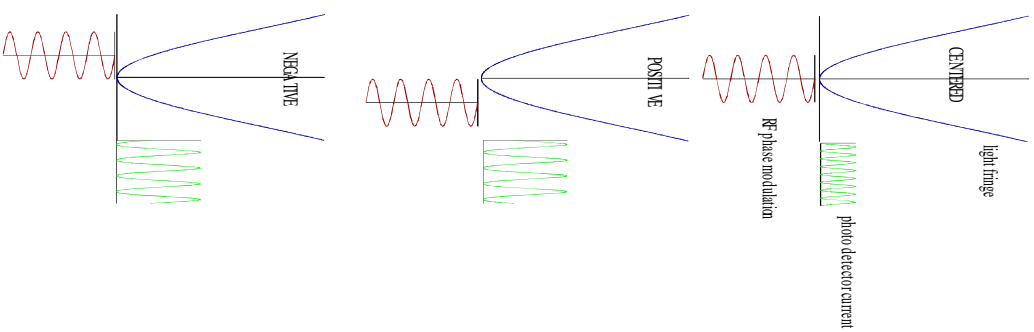
arm length = 4000 m

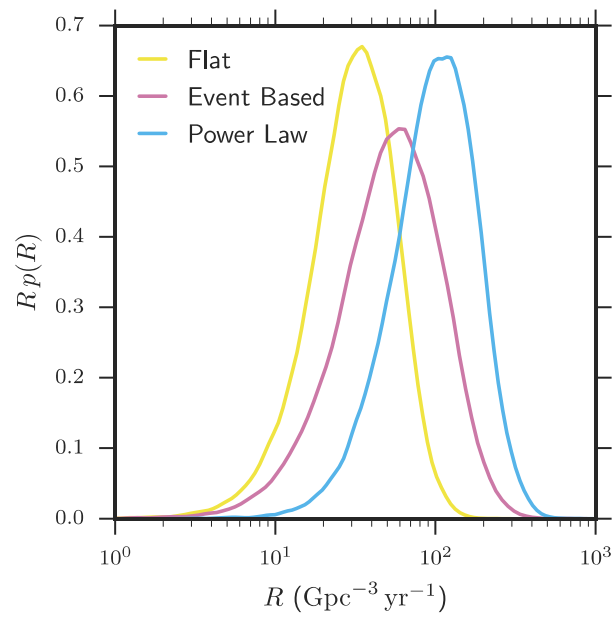
equivalent # of passes = 100

integration time

number of quanta/second at the beam splitter
 300 watts at beam splitter = 10^{21} identical photons/sec

$h = 6 \times 10^{-22}$ integration time 10^{-2} sec





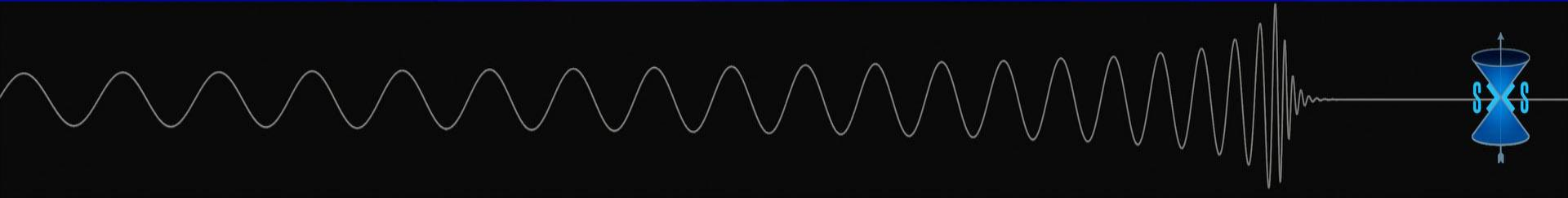
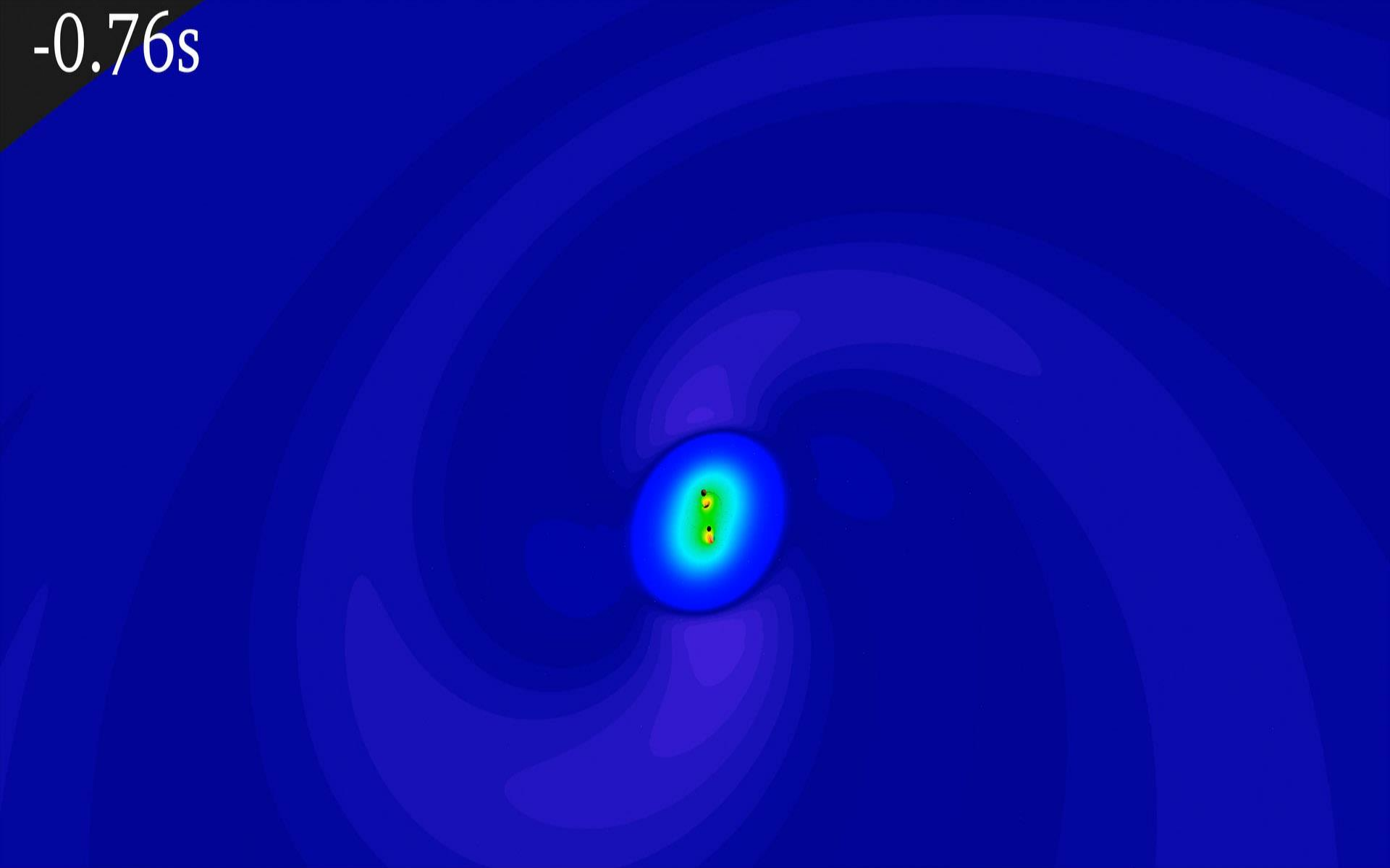




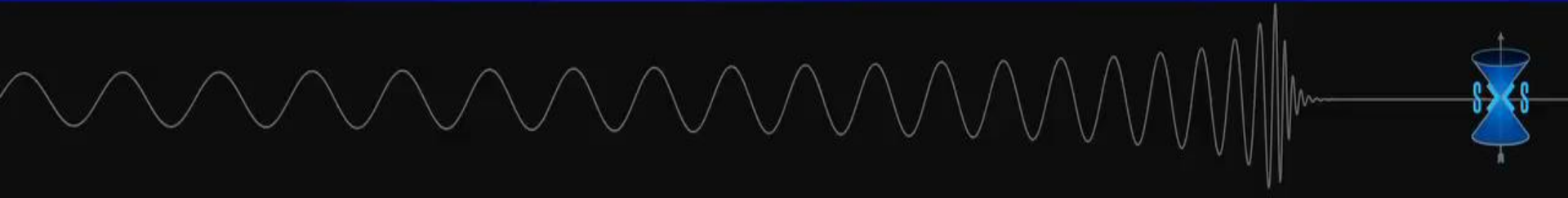
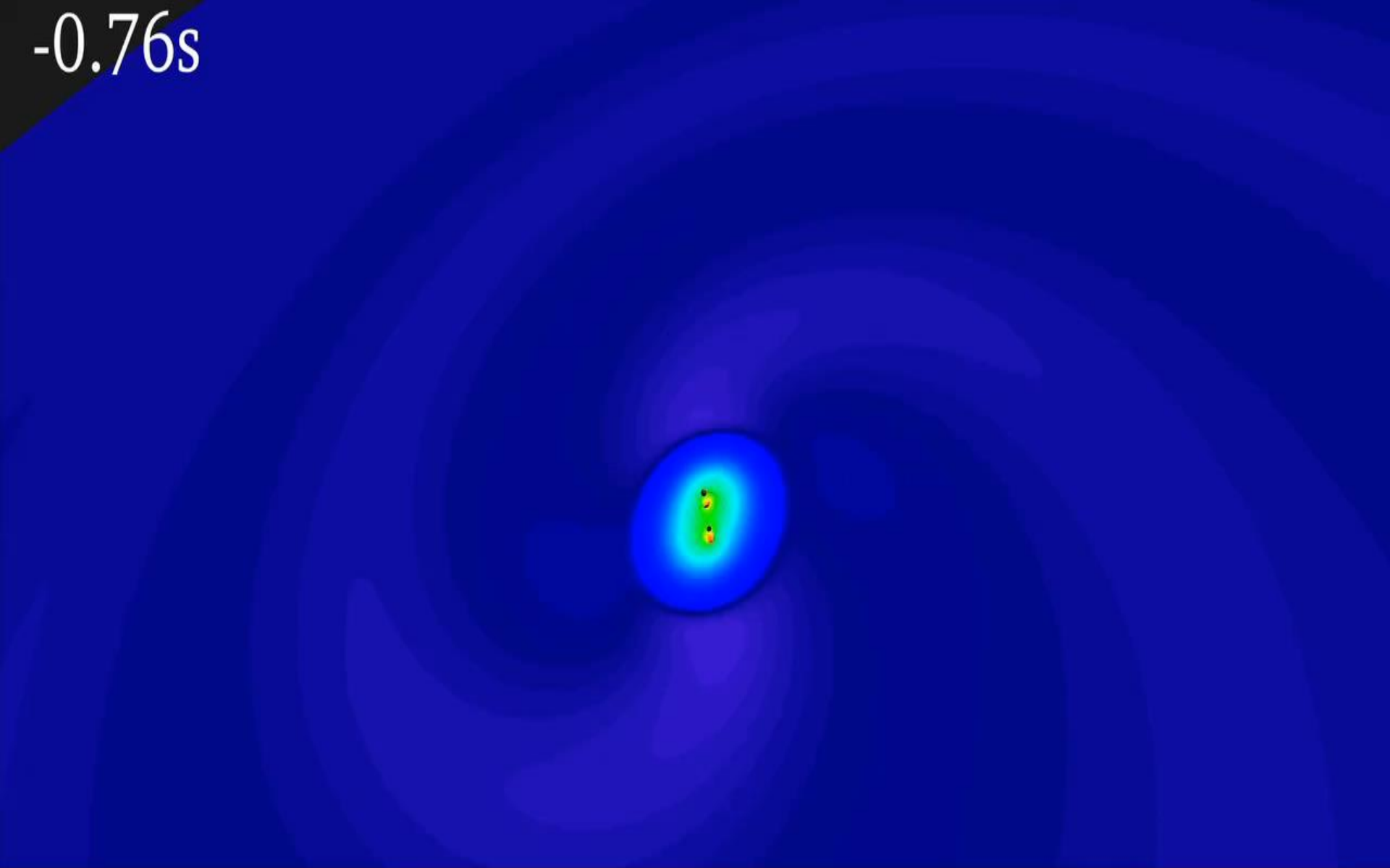
How Small is 10^{-18} Meter?

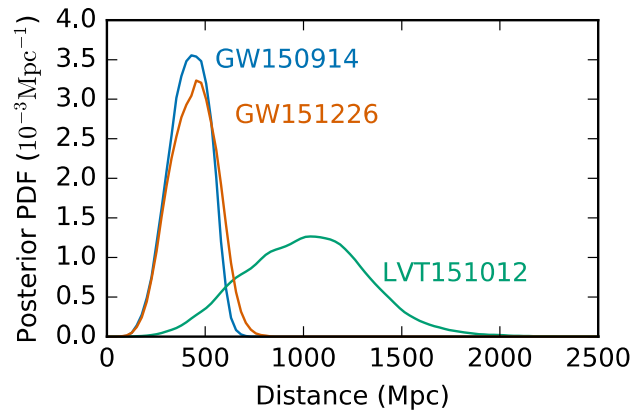
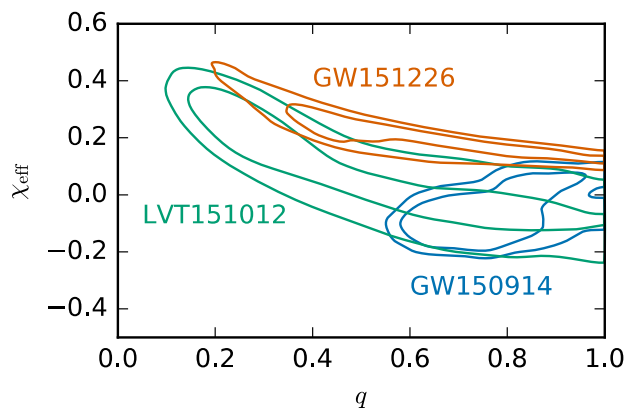
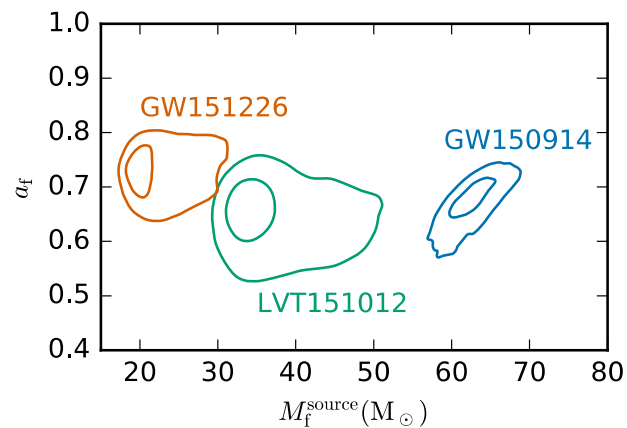
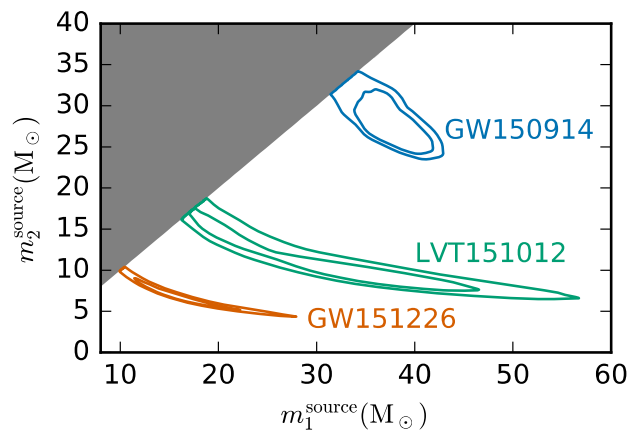
		<i>One meter, about 40 inches</i>
$\div 10,000$		<i>Human hair, about 100 microns</i>
$\div 100$		<i>Wavelength of light, about 1 micron</i>
$\div 10,000$		<i>Atomic diameter, 10^{-10} meter</i>
$\div 100,000$		<i>Nuclear diameter, 10^{-15} meter</i>
$\div 1,000$		<i>LIGO sensitivity, 10^{-18} meter</i>

-0.76s



-0.76s





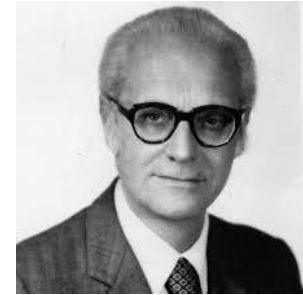
Acoustic bar GW Detector groups



R. Garwin



W. Fairbank



E. Amaldi

1965-1975 Room T bars

Bell Labs
Frascati
Glasgow
IBM
Rochester
Max Planck
Rome

1975-1990+ Cryogenic bars

Frascati
Louisiana
Moscow
Perth
Rochester
Stanford

2000 -> Spherical cryogenic detectors

Brazil
Netherlands



A. Tyson



W. Hamilton



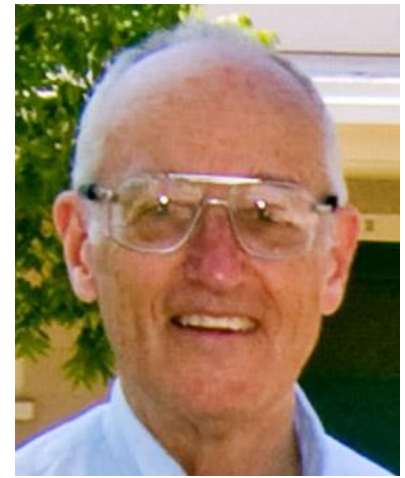
P. Michelson

Stanford Contributions to LIGO

1.06 micron solid state frequency
and amplitude stabilized laser
(1986)



Robert Byer



Dan DeBra

Active hydraulic seismic
isolation system (2000)



Peter Michelson



Brian Lantz

Advanced Detector active
seismic isolation system
(2010)



Marty Fejer



Brett Shapiro

Low thermal noise optical
coating research (2017)